One-dimensional lattice random walks in a Gaussian random potential

Journal of Physics A: Mathematical and Theoretical

OPEN ACCESS

RECEIVED
19 March 2026

REVISED
27 June 2026

ACCEPTED FOR PUBLICATION
28 July 2026

PUBLISHED
17 August 2026

PAPER

One-dimensional lattice random walks in a Gaussian random potential

Silvio Kalaj[1,2,*], **Enzo Marinari**[1,3], **Gleb Oshanin**[2] and **Luca Peliti**[4]

[1] Dipartimento di Fisica, Sapienza Università di Roma, P.le A. Moro 2, I-00185 Roma, Italy
[2] Sorbonne Université, CNRS, Laboratoire de Physique Théorique de la Matière Condensée (UMR 7600), 4 Place Jussieu, 75252 Paris Cedex 05, France
[3] INFN, Sezione di Roma 1 and Nanotech-CNR, UOS di Roma, P.le A. Moro 2, I-00185 Roma, Italy
[4] Santa Marinella Research Institute, I-00058 Santa Marinella, Italy
[*] Author to whom any correspondence should be addressed.

E-mail: silvio.kalaj@gmail.com

Keywords: random walks in disordered media, Gaussian random potential, self-averaging vs non-self-averaging

Abstract

We study random walks evolving in continuous time on a one-dimensional lattice where each site x hosts a quenched random potential U_x. The potentials on different sites are independent, identically distributed Gaussian random variables. We analyze three distinct models that specify how the transition rates depend on U_x: the random-force-like model, random walks with randomized stepping times, and the Gaussian trap model. Our analysis focuses on five key disorder-dependent quantities defined for a finite chain with N sites: the probability current, its reciprocal (the resistance), the splitting probability E_-, the mean first-passage time T_N, and the diffusion coefficient D_N in a periodic chain. By determining the moments of these random variables, we demonstrate that the probability current and resistance are not self-averaging, which leads to pronounced differences between their average and typical behaviors. In contrast, E_-, T_N and D_N become self-averaging when $N \to \infty$, though they exhibit strong sample-to-sample fluctuations for finite N.

1. Introduction

Understanding the various aspects of a particle's random motion in disordered environments presents a significant challenge, stemming from both mathematical and physical complexities, as well as a wide range of practical applications. In many real-world systems, the medium through which a particle moves is highly irregular, influenced by defects, impurities, fluctuations, and other factors. These irregularities create a random environment that affects local transition rates and often alters the behavior of averaged transport characteristics. Since the early studies that introduced several foundational results, along with various analytical approaches (see, for example, [1–10]), substantial progress has been made across different areas of this vast domain. Notable topics include diffusion in random forcing landscapes [11–22], in the presence of quenched random traps (see, e.g., [23–32]), random stratified flows [34–36], and flows on various types of random lattices [37, 38]. The impact of disorder—such as sequence heterogeneity—on random transport in biological systems has been studied in various contexts. These include polynucleotide translocation through nanopores, the movement of molecular motors or proteins along DNA [39–42], the dynamics of twist-induced denaturation bubbles in long DNA strands [43], and the behavior of the boundary between coil and ordered helix phases during heteropolymer melting [44] (see also [45]). A rich body of results and concepts has been summarized in several comprehensive reviews [46–52]. Despite this progress, the problem remains a vibrant area of research, with many aspects still not fully understood and being the subject of ongoing studies. For example, recent papers have examined the influence of correlated disorder on transport properties [53], the dynamics of active particles such as bacteria in disordered environments [54–58], and sequence-reading diffusion model that mimics in some effective way the random translocation of knots along chemically heterogeneous DNA strands [59].

In this paper, we revisit the long-standing problem of random walks in the presence of a quenched random Gaussian potential (Gaussian white noise), a topic that has received a significant attention in the past (see, e.g., [51]). Specifically, we study dynamics of a particle that undergoes, in continuous time, a random walk between nearest-neighboring sites of a one-dimensional lattice, where each site x hosts a quenched random potential U_x, which influences the local transition rates. The variables U_x are independent and identically distributed (iid) random variables, with a common Gaussian distribution. This model can be also viewed from a somewhat different perspective. Namely, it can be considered as an effective description, in terms of the Fick-Jacob's approximation (see, e.g., [60, 61]), of diffusion in a narrow two- or three-dimensional channel with Gaussian-distributed random wall corrugation.

To define the transition rates as functions of the on-site potentials, we consider three distinct scenarios: (a) the 'random force'-like model [49], (b) a continuous-time random walk (CTRW) [62] with an exponential waiting-time distribution and the transition probabilities dependent on the values of potentials at the neighboring sites, and (c) a Gaussian random trap model (see, e.g., [23–33, 49]). We will provide a more detailed definition of the dynamics for all three models in the following sections.

Our analysis focuses on five *realization-dependent* random variables:

(a) The steady-state probability current through a finite chain consisting of N sites.

(b) Its reciprocal value, which represents the resistance of a finite interval with N sites with respect to a random transport.

(c) The splitting probability—the probability that the particle starting at the site x_0 in a finite interval $(0, N)$ reaches the left extremity of the interval first, without ever visiting the right end of the interval.

(d) The mean first-passage time through a finite interval of length N.

(e) The diffusion coefficient in a finite periodic chain with N sites.

While the statistics of the last two quantities have been explored in previous studies and some well-established results have been obtained (see, e. g., [48, 49, 51]), a comprehensive analysis of the first three variables is lacking at present. It is also important to note that all the random variables under study are formally defined in the limit $t \to \infty$. Consequently, our analysis does not address transient effects, such as aging and the ensuing sub-diffusive behavior, which have been extensively discussed in the literature on the random force and random traps models (see, e. g., [49]).

Our objective is to calculate the leading asymptotic forms of the moments of these random variables in the large-N limit, as well as to understand how they depend on the strength of disorder. For intermediate values of N, we will conduct numerical analyses, employing exact numerical averaging of the formal expressions that define these properties for a given sequence of U_x values. Ultimately, we aim to address a conceptually important question whether these transport properties exhibit self-averaging with respect to different realizations of disorder in the limit $N \to \infty$. In quest for the answer, we will examine the large-N asymptotic forms of the key parameter—the relative variance

$$R_\zeta = \frac{\langle \zeta^2 \rangle - \langle \zeta \rangle^2}{\langle \zeta \rangle^2}, \tag{1}$$

where the angle brackets here and henceforth denote averaging with respect to realizations of disorder, while ζ is one of the above-mentioned random variables of interest. This parameter establishes a standard criterion (see, for example, [64]) that allows us to conclude whether the realization-dependent random variable ζ is self-averaging ($R_\zeta \to 0$ as $N \to \infty$) or not ($R_\zeta \to$ const as $N \to \infty$). Determining which of the two possible outcomes is realized is of a considerable conceptual importance: in a self-averaging system, a single sufficiently large sample can provide a representative insight into the behavior of the entire statistical ensemble. Conversely, in the absence of self-averaging, the value of an observable derived from a single, even large, sample will not be representative and must be assessed from an ensemble of samples. Consequently, one may expect a much more significant scatter of the data for a single realization of disorder in the latter than in the former case. It is also important to note that for finite N, the relative variance R_ζ is always greater than zero, indicating that fluctuations are significant for finite samples. Note as well that the limit $N \to \infty$ itself is very meaningful for the diffusion coefficient, as it reflects the behavior expected in infinite systems. In contrast, for other properties of interest, this limit will only highlight a trend in the behavior of fluctuations. Specifically, for quantities such as currents, resistances, splitting probabilities, and the mean first-passage times, the size N remains fundamentally finite.

The paper is outlined as follows: In section 2 we present our model and describe three different dynamical scenarios. In section 3 we concentrate on the statistical properties of the realization-dependent currents through a finite chain and of its reciprocal value—the resistance of a finite chain with respect to a random transport. In section 4 we discuss the behavior of the realization-dependent splitting probabilities. Section 5 is devoted to the analysis of the mean first-passage times through finite intervals. Next, in section 6 we evaluate the moments of the diffusion coefficient in period chains in the limit $N \to \infty$ for all three dynamical scenarios. In section 7 we conclude with a brief recapitulation of our results. Some derivations are relegated to Appendices. In appendix A we present the derivation of the probability currents through a finite chain with fixed disorder for all three dynamical scenarios, while in appendix B we express the realization-dependent splitting probability through the resistances of the intervals from the right and from the left of the starting point $x = x_0$. Lastly, in appendix C, capitalizing on the exact result due to Derrida [4], we derive exact compact expressions for the realization-dependent diffusion coefficient on a periodic chain for all three dynamical scenarios.

2. Model and dynamical scenarios

Consider a one-dimensional regular lattice with inter-site spacing a. Without loss of generality, we set $a = 1$ in what follows. We assign to each site x (x is an integer) of this lattice a quenched random variable U_x and assume that all U_x-s are independent, identically distributed (iid) random variables with the common Gaussian distribution. When U_x are defined on the entire real line, $-\infty < U_x < \infty$, we have

$$P(U) = \frac{1}{\sqrt{2\pi\sigma^2}} \exp\left(-\frac{U^2}{2\sigma^2}\right), \tag{2}$$

while if U_x may attain only negative real values[5], $-\infty < U_x \leqslant 0$, the probability density function of U_x obeys

$$P_-(U) = \sqrt{\frac{2}{\pi\sigma^2}} \exp\left(-\frac{U^2}{2\sigma^2}\right). \tag{3}$$

In what follows we will also use auxiliary variables ϕ_x, defined as

$$\phi_x = \exp\left(\frac{\beta U_x}{2}\right), \tag{4}$$

which will permit us to somewhat ease the notations and also to write down all the properties under study, which are functionals of a set of all ϕ_x-s, in a very compact and transparent way. For Gaussian iid variables U_x, the variables ϕ_x are also iid random variables with the common log-normal probability density function. For U_x defined on the entire axis

$$P(\phi) = \sqrt{\frac{2}{\pi\beta^2\sigma^2}} \frac{1}{\phi} \exp\left(-\frac{2}{\beta^2\sigma^2} \ln^2(\phi)\right), \quad 0 \leqslant \phi < \infty, \tag{5}$$

while for $-\infty < U_x \leqslant 0$ we have

$$P_-(\phi) = \sqrt{\frac{8}{\pi\beta^2\sigma^2}} \frac{1}{\phi} \exp\left(-\frac{2}{\beta^2\sigma^2} \ln^2(\phi)\right), \quad 0 \leqslant \phi \leqslant 1. \tag{6}$$

In both cases the variables ϕ_x have finite moments of *arbitrary* positive or negative (not necessarily integer) order q.

The random walk of a particle in such a random frozen environment is defined using three different scenarios.

2.1. Scenario I: random force-like model

Here we follow the rules of the so-called 'random force' model (see, e.g., [49] for a review) defining on each link that connects sites x and $x+1$ a random force $F_{x,x+1} = -(U_{x+1} - U_x)/a$, ($a = 1$). Note that this force varies randomly from site to site, but is not statistically *independent* from the forces defined on two neighboring sites, as it is the case in, e.g., the Temkin or Sinai models [11–22]. In our setting

[5] See below the definition of the Gaussian random trap model.

the random force is the difference of two on-site potentials, which are the iid random variables[6]. More importantly, in stark contrast to the Temkin and Sinai models, the disorder landscape in our case does not become progressively rougher with increasing system size. Consequently, neither the typical heights of potential barriers nor the depths of potential wells grow with the size of the system, which leads to fundamentally different large-scale dynamical behavior. We stipulate then that the particle performs activated hopping motion in a continuous-time between the nearest-neighboring sites with the transition rates $W_{x,x+1}$ and $W_{x,x-1}$ from the host site x to the target sites $x+1$ or $x-1$, respectively, which obey

$$\begin{aligned} W_{x,x\pm1} &= W_0 \exp\left(\frac{\beta}{2}\left(U_x - U_{x\pm1}\right)\right) = W_0 \frac{\phi_x}{\phi_{x\pm1}}\,, \\ W_{x\pm1,x} &= W_0 \exp\left(\frac{\beta}{2}\left(U_{x\pm1} - U_x\right)\right) = W_0 \frac{\phi_{x\pm1}}{\phi_x}\,, \end{aligned} \tag{7}$$

where β is the reciprocal temperature measured in units of the Boltzmann constant, while W_0 is the characteristic rate which defines the frequency of jumps in absence of disorder. In this scenario, the probability $P_x(t)$ of finding the particle at site x at time instant t obeys the master equation

$$\dot{P}_x(t) = W_{x+1,x}P_{x+1}(t) + W_{x-1,x}P_{x-1}(t) - \left(W_{x,x+1} + W_{x,x+1}\right)P_x(t)\,, \tag{8}$$

where the dot denotes the time derivative. Such a model evidently satisfies detailed balance and, on a finite periodic chain with N sites, $x = 1, 2, \ldots, N$, the normalized position probability P_x evolves towards an equilibrium state with

$$P_x(t=\infty) = \frac{\exp(-\beta U_x)}{\sum_{y=1}^{N}\exp(-\beta U_y)} = \frac{\phi_x^{-2}}{\sum_{y=1}^{N}\phi_y^{-2}}\,. \tag{9}$$

2.2. Scenario II: random walk with randomized stepping-times

We aim now to work out a somewhat different dynamical scenario which yields a continuous-time master equation with the normalized transition *probabilities*, rather than the rates. To this end, consider first an auxiliary random walk problem in which a particle steps at each tick $n = 1, 2, 3, \ldots$ of the clock between the nearest-neighboring sites of a lattice of integers x. The probability $P_x(n)$ of finding the particle at site x at discrete time moment n is governed by a general equation for a random walk [50] :

$$P_x(n) = p_{x+1,x}P_{x+1}(n-1) + p_{x-1,x}P_{x-1}(n-1)\,, \tag{10}$$

where $p_{x+1,x}$ and $p_{x-1,x}$ are (time-independent) probabilities that a particle hops from the site $x+1$ or from the site $x-1$, respectively, to the site x. The probabilities of hops from the site x to either of the neighboring sites are normalized, $p_{x,x+1} + p_{x,x-1} = 1$, such that the particle cannot pause at x.

Recalling that each site of the lattice hosts a random potential U_x, we define the transition *probabilities* $p_{x,x\pm1}$ in the way which resembles the definition of the transition rates in the above Model I, except that these probabilities are normalized to unity. That being, we stipulate that

$$\begin{aligned} p_{x,x+1} &= Z_x^{-1}\exp\left(\frac{\beta}{2}\left[U_x - U_{x+1}\right]\right)\,, \\ p_{x,x-1} &= 1 - p_{x,x+1} = Z_x^{-1}\exp\left(\frac{\beta}{2}\left[U_x - U_{x-1}\right]\right)\,, \end{aligned} \tag{11}$$

where Z_x is the normalization,

$$Z_x = \exp\left(\frac{\beta}{2}\left[U_x - U_{x+1}\right]\right) + \exp\left(\frac{\beta}{2}\left[U_x - U_{x-1}\right]\right)\,. \tag{12}$$

The transition probabilities $p_{x,x+1}$ and $p_{x,x-1}$ in equation (11) can be also conveniently expressed through auxiliary variables ϕ_x in equation (4) to give

$$p_{x,x+1} = \frac{\phi_{x-1}}{\phi_{x-1} + \phi_{x+1}}\,, \quad p_{x,x-1} = \frac{\phi_{x+1}}{\phi_{x-1} + \phi_{x+1}}\,. \tag{13}$$

[6] To prevent any confusion, we refer therefore to this dynamic scenario as the 'random-force-like' model, since the term 'random-force' model is typically reserved for situations in which the forces themselves are independent and identically distributed random variables.

Note that the definition of the transition probabilities in equation (11) is essentially the same as in the 'random walk on a random hillside' model [6, 7], except that in the latter the potential of the target site is taken in the middle of the link connecting the host and the target sites. In our model the transition probabilities involve the values of potentials on the host and the target sites themselves.

Before we proceed, it might be also instructive to formally rewrite equations (11) as

$$p_{x,x+1} = \frac{1}{1+\exp\left(-\beta F_{x-1,x+1}\right)}, \quad p_{x,x-1} = \frac{1}{1+\exp\left(\beta F_{x-1,x+1}\right)}, \tag{14}$$

where $F_{x-1,x+1} = -(U_{x+1} - U_{x-1})/2$ can be identified as the force acting on the particle being at site x. In this way, the particle being at site x 'feels' only the values of potentials at two adjacent sites and the probability to jump towards the neighboring site with a lower energy is bigger than the probability to make a jump in the opposite direction, regardless of the actual value of U_x.

We turn to a *randomized stepping-time* version of the above model, which will be our Model II. We suppose now that the random walk evolves in continuous-time and in each realization of the process the particle steps from the site it occupies at random time instants t_1, t_2, $t_3, \ldots$, where the time-intervals $\triangle_1 = t_1 - t_0$, $(t_0 = 0)$, $\triangle_2 = t_2 - t_1$, $\triangle_3 = t_3 - t_2$, …, are iid random variables with the probability density function

$$P(\triangle) = \exp\left(-\frac{\triangle}{\delta t}\right)/\delta t. \tag{15}$$

The sequence t_1, t_2, $t_3, \ldots$ is therefore a Poisson point process with density $P(\triangle)$ and the mean value of the time-interval between the successive steps is equal to δt, such that the ensuing hopping process is simply the Montroll–Weiss CTRW [62] (see also [50] for an overview) in which the waiting times are iid random variables with an exponential distribution.

To define the time-evolution of the position probability $P_x = P_x(t)$ for Model II, we take advantage of the analysis in [63] (see also [50]), which showed that for any value of time t the time-evolution of the latter probability for the above-defined CTRW is governed, in place of the discrete-time equation (10), by the master equation of the form:

$$\delta t \dot{P}_x(t) = p_{x-1,x}P_{x-1}(t) + p_{x+1,x}P_{x+1}(t) - P_x(t), \tag{16}$$

where the transition probabilities are defined in equation (11) (or equation (14)). The master equation (16) is Markovian, as the one for the Model I, so that the future evolution is sensitive only to the present state while detailed history is irrelevant. At first glance, this may seem somewhat surprising because in the CTRW the particle steps at random time instants and therefore, there is a memory (albeit a short-ranged) on the time instant when the previous stepping event took place. As shown in [63], a Poisson point process with the density $P(\triangle)$ in equation (15) is a *unique* example of a stochastic stepping process for which the Markovian master equation (16), corresponding to the process in equation (10) with randomized stepping times, is exact.

Note, as well, that equation (16) evidently satisfies detailed balance and its stationary solution on a periodic chain with N sites (see [73] for the definition of $P_x(t=\infty)$ in terms of the transition probabilities or rates) has a bit more complicated form than the one in equation (9). For any given sequence of U_x it reads

$$\begin{aligned} P_x(t=\infty) &= \frac{1}{2}\left(\exp\left(-\frac{\beta}{2}(U_{x-1}+U_x)\right) + \exp\left(-\frac{\beta}{2}(U_x+U_{x+1})\right)\right) \\ &\quad \times \left(\sum_{y=1}^{N}\exp\left(-\frac{\beta}{2}(U_y+U_{y+1})\right)\right)^{-1} \\ &= \frac{1}{2}\left(\frac{1}{\phi_{x-1}\phi_x} + \frac{1}{\phi_x\phi_{x+1}}\right)\left(\sum_{y=1}^{N}\frac{1}{\phi_x\phi_{x+1}}\right)^{-1}, \end{aligned} \tag{17}$$

with $U_{N+1} = U_1$ and $\phi_{N+1} = \phi_1$.

We finally remark that although the master equations (8) and (16) have quite different forms, they reduce to the same conventional Fokker–Planck equation when one turns to the continuous-space limit.

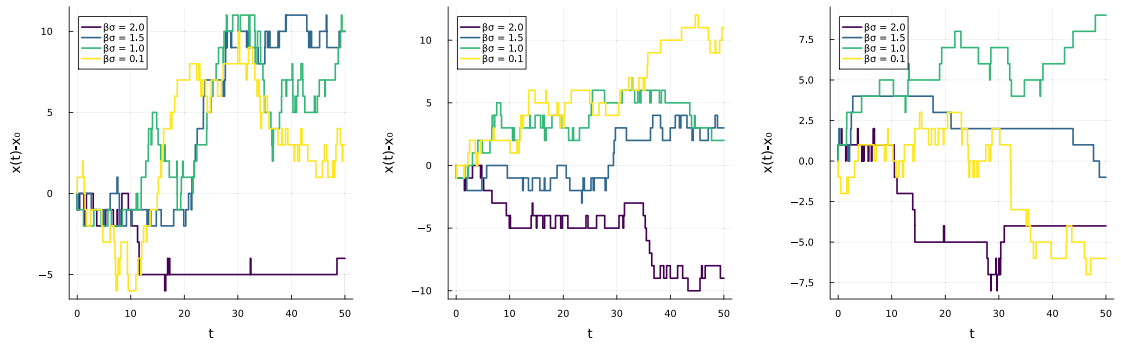

Figure 1. Four individual short trajectories for the Model I (left panel), Model II (middle panel) and Model III (right panel) for four values of the parameter $\beta\sigma$ (see the inset).

Rewriting equations (8) and (16) for the lattices with an inter-site spacing a and then setting $a \to 0$, one finds via a standard procedure that $P_x(t)$ obeys

$$\dot{P}_x(t) = D\frac{\mathrm{d}}{\mathrm{d}x}\left(\frac{\mathrm{d}}{\mathrm{d}x}P_x(t) + \beta P_x(t)\frac{\mathrm{d}U_x}{\mathrm{d}x}\right), \tag{18}$$

where the diffusion coefficient $D = W_0 a^2$ and $D = a^2/2\delta t$ for the Model I and the Model II, respectively. Both diffusion coefficients are assumed to be finite in the limit $a \to 0$, $W_0 \to \infty$ and $\delta t \to 0$. In this limit, the expressions (9) and (17) for the probabilities of being at site x at time $t \to \infty$ in both Models coincide and are given by the stationary solution of equation (18) in a box of size L,

$$P_x(t=\infty) = \frac{\exp\left(-\beta U_x\right)}{\int_0^L \mathrm{d}x \exp\left(-\beta U_x\right)}. \tag{19}$$

At the same time, given the difference between the master equations (8) and (16), we may expect that the behavior of the above-mentioned disorder-dependent random variables for finite inter-site spacing a will be different for the two models under study. In figure 1, in the left and middle panels, we depict four trajectories generated using the standard Gillespie algorithm [74] for the Models I and II, respectively, for four values of the parameter $\beta\sigma$, which indeed show quite a different behavior for the same values of $\beta\sigma$. The difference becomes more pronounced the larger $\beta\sigma$ is.

2.3. Scenario III: Gaussian random trap model

In the third scenario, we use the so-called random trap model (see [23–33, 49]), which offers a simplified yet physically plausible framework for studying slow dynamics, aging and anomalous diffusion in disordered media. This includes systems such as glasses, spin glasses, disordered solids or other complex systems characterized by rugged energy landscapes featuring multiple local minima of random depths. In this context, we assume that each site x hosts a trap with a depth $-U_x$, U_x being a quenched, negative definite random variable with the Gaussian probability density function in equation (3). The values of the depths of traps at different sites are uncorrelated. The particle undergoes activated hopping motion on this lattice and the time it spends in the trap at site x is governed by the Arrhenius law, meaning that this time is proportional to $\exp(-\beta U_x)$.

The time evolution of the probability $P_x = P_x(t)$ of finding the particle at site x at a given time instant t follows the master equation (8) with the transition rates

$$W_{x,x\pm1} = W_0\,\mathrm{e}^{\beta U_x} = W_0\phi_x^2. \tag{20}$$

Notably, the transition rates in this framework depend solely on the depth of the trap at the host site x and are unaffected by the values $U_{x\pm1}$ that characterize the traps at the neighboring target sites. Such a model also satisfies detailed balance and on a finite periodic chain with N sites, $x = 1, 2, \ldots, N$, the position probability P_x approaches an equilibrium value as defined in equation (9), mirroring the behavior observed in the Model I. In contrast, in the continuous-space limit P_x does not obey the Fokker–Planck equation in equation (18). Instead, it follows a Fokker–Planck equation with a position-dependent diffusion coefficient. Four individual particle's trajectories generated for the discrete-space Gaussian random trap model are depicted in the right panel in figure 1 and show a markedly different behavior for sufficiently large values of $\beta\sigma$ as compared to the one observed in Models I and II.

3. The realization-dependent currents and the resistances

Consider a finite chain of sites $x = 0, 1, 2, \ldots, N$ with a fixed sequence of U_x-s. At site $x = 0$ we introduce a source of particles which maintains a constant occupation of this site, $P_0 = c_0$, while at the opposite extremity of the chain, i.e., at $x = N$, we place a perfect sink which removes particles from the system, $P_N = 0$. Such a system evolves towards a steady-state with a constant current j_N to the sink, which is the following functional of a given sequence of U_x-s (see [59] and appendix A for more details) :

$$j_N^{(I)} = \frac{W_0 c_0}{\tau_N^{(I)}}, \quad j_N^{(II)} = \frac{c_0}{2\delta t \tau_N^{(II)}}, \quad j_N^{(III)} = \frac{W_0 c_0}{\tau_N^{(III)}}, \tag{21}$$

where the superscript indicates the dynamical scenario, while $\tau_N^{(I)}$, $\tau_N^{(II)}$ and $\tau_N^{(III)}$ are the corresponding to each scenario realization-dependent resistances of a finite chain. The identification of these quantities as effective electrical resistances relies on the well-known isomorphism between Markov chains and resistor networks, a connection extensively detailed in [75]. They are explicitly given by (see appendix A)

$$\tau_N^{(I)} = \frac{H_{0,N}}{\phi_0^2}, \quad \tau_N^{(II)} = \frac{H_{0,N}}{\phi_0 \phi_1}, \quad \tau_N^{(III)} = \frac{N}{\phi_0^2}, \tag{22}$$

where $H_{0,N}$ is the following functional

$$H_{0,N} = \phi_0\phi_1 + \phi_1\phi_2 + \phi_2\phi_3 + \phi_3\phi_4 + \ldots + \phi_{N-2}\phi_{N-1} + \phi_{N-1}\phi_N. \tag{23}$$

In the latter expression the subscript 0 corresponds to the first site in the sequence, i.e., $x = 0$, while the subscript N—to the last site $x = N$.

3.1. The moments of resistances

The first two moments of the realization-dependent resistances of the discrete-space finite chains can be straightforwardly calculated in the leading in the large N limit order, to give

$$\begin{aligned} \left\langle \tau_N^{(I)} \right\rangle &= \langle \phi \rangle^2 \left\langle \frac{1}{\phi^2} \right\rangle N + O(1) = \exp\left(3\beta^2\sigma^2/4\right) N + O(1), \\ \left\langle \left(\tau_N^{(I)}\right)^2 \right\rangle &= \langle \phi \rangle^4 \left\langle \frac{1}{\phi^4} \right\rangle^2 N^2 + O(N) = \exp\left(5\beta^2\sigma^2/2\right) N^2 + O(N), \end{aligned} \tag{24}$$

$$\begin{aligned} \left\langle \tau_N^{(II)} \right\rangle &= \langle \phi \rangle^2 \left\langle \frac{1}{\phi} \right\rangle^2 N + O(1) = \exp\left(\beta^2\sigma^2/2\right) N + O(1), \\ \left\langle \left(\tau_N^{(II)}\right)^2 \right\rangle &= \langle \phi \rangle^4 \left\langle \frac{1}{\phi^2} \right\rangle^2 N^2 + O(N) = \exp\left(3\beta^2\sigma^2/2\right) N^2 + O(N), \end{aligned} \tag{25}$$

and

$$\begin{aligned} \left\langle \tau_N^{(III)} \right\rangle &= \left\langle \frac{1}{\phi^2} \right\rangle N = \exp\left(\beta^2\sigma^2/2\right) \left(1 + \mathrm{erf}\left(\beta\sigma/\sqrt{2}\right)\right) N, \\ \left\langle \left(\tau_N^{(III)}\right)^2 \right\rangle &= \left\langle \frac{1}{\phi^4} \right\rangle N^2 = \exp\left(2\beta^2\sigma^2\right) \left(1 + \mathrm{erf}\left(\sqrt{2}\beta\sigma\right)\right) N^2, \end{aligned} \tag{26}$$

where the symbols $O(1)$ and $O(N)$ signify that the omitted terms are independent of N and are linear with N, respectively, while $\mathrm{erf}(x)$ denotes the error function. In equations (24) and (25) the averaging is performed with respect to the probability density function (5), while the moments of $\tau_N^{(III)}$ are evaluated by using the analogous function in equation (6). Note that the moments of the resistances $\tau_N^{(I)}$ and $\tau_N^{(II)}$ exhibit a super-Arrhenius dependence on the temperature for any value of the parameter $\beta\sigma$, while the moments of $\tau_N^{(III)}$ show the super-Arrhenius behavior only for $\beta\sigma \to \infty$, in which limit $\left\langle \tau_N^{(III)} \right\rangle \simeq 2\exp(\beta^2\sigma^2/2)N$. For small values of $\beta\sigma$, in the Taylor series expansion of $\tau_N^{(III)}$ the first subdominant term is linear with $\beta\sigma$,

$$\left\langle \tau_N^{(III)} \right\rangle \simeq \left(1 + \sqrt{\frac{2}{\pi}}\beta\sigma + \frac{\beta^2\sigma^2}{2} + O\left(\beta^3\sigma^3\right)\right) N. \tag{27}$$

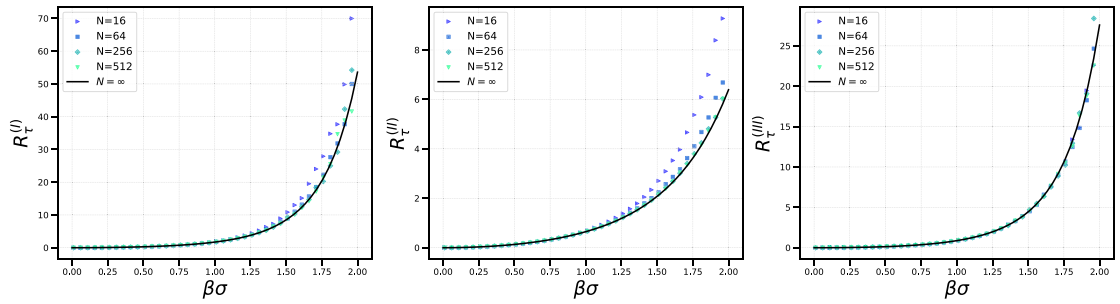

Figure 2. The relative variances R_τ of the resistances τ_N in the Models I (left panel), II (middle panel) and III (right panel) as functions of $\beta\sigma$. Solid curves are our analytical predictions in equations (28) to (30) for $N=\infty$, while the symbols depict R_τ evaluated by a numerical averaging of τ_N and τ_N^2 for finite values of N (see the insets).

From equations (24) and (25) we find that the corresponding relative variances in equation (1) obey

$$R_{\tau^{(I)}} = \left\langle \left(\tau_N^{(I)}\right)^2 \right\rangle \Big/ \left\langle \tau_N^{(I)} \right\rangle^2 - 1 = \exp\left(\beta^2\sigma^2\right) - 1 + O(1/N)\,, \tag{28}$$

$$R_{\tau^{(II)}} = \left\langle \left(\tau_N^{(II)}\right)^2 \right\rangle \Big/ \left\langle \tau_N^{(II)} \right\rangle^2 - 1 = \exp\left(\beta^2\sigma^2/2\right) - 1 + O(1/N)\,, \tag{29}$$

while for the Model III the relative variance is independent of N and is given by a more complicated expression of the form

$$R_{\tau^{(III)}} = \left\langle \left(\tau_N^{(III)}\right)^2 \right\rangle \Big/ \left\langle \tau_N^{(III)} \right\rangle^2 - 1 = \frac{\left(1+\mathrm{erf}\left(\sqrt{2}\,\beta\sigma\right)\right)}{\left(1+\mathrm{erf}\left(\beta\sigma/\sqrt{2}\right)\right)^2} \exp\left(\beta^2\sigma^2\right) - 1\,. \tag{30}$$

The above equations (28) and (29) imply that the resistances in Models I and II are *not self-averaging* in the limit $N\to\infty$. The resistance in the Model III is not self-averaging for any value of N. Moreover, in all three Models the relative variances R_τ show an unbounded growth with $\beta\sigma$, which signifies that fluctuations become more important the larger the disorder is. The behavior of R_τ for all three Models is depicted in figure 2. Below we will show that such a lack of self-averaging is essentially the boundary effect.

3.2. The limit distributions of the resistances and their typical values

To get an idea why the resistances are not self-averaging in all three Models, we seek their probability density functions. We start with Model I. The limiting for $N\to\infty$ form of the probability density function of $\tau_N^{(I)}$ can be evaluated following the standard approach: We first consider a reduced random variable

$$\overline{\tau}_{(I)} = \frac{\tau_N^{(I)}}{N}\,, \tag{31}$$

and focus on the form of its moment-generating function in the limit $N\to\infty$,

$$\Phi(\overline{\tau}_{(I)}) = \lim_{N\to\infty} \left\langle \exp\left(-\lambda\overline{\tau}_{(I)}\right) \right\rangle, \quad \lambda \geqslant 0\,, \tag{32}$$

where the angle brackets denote the averaging over all random variables ϕ_x. Once $\Phi(\overline{\tau}_{(I)})$ is known, the probability density function $P(\overline{\tau}_{(I)})$ obtains by a mere inversion of the Laplace transform.

We formally split the averaging over all sites in equation (32) into the averaging over the variables ϕ_x for all the 'bulk' sites $x=1,2,3,\ldots,N$, and the averaging over the variable ϕ_0, such that

$$\begin{aligned}\Phi(\overline{\tau}_{(I)}) &= \lim_{N\to\infty} \left\langle \left\langle \exp\left(-\lambda\overline{\tau}_{(I)}\right) \right\rangle_{\mathrm{bulk}} \right\rangle_0 \\ &= \lim_{N\to\infty} \left\langle \left\langle \exp\left(-\frac{\lambda}{N\phi_0^2} H_{0,N}\right) \right\rangle_{\mathrm{bulk}} \right\rangle_0\,,\end{aligned} \tag{33}$$

We notice next that $H_{0,N}$ in equation (23) is self-averaging. Indeed, we have

$$\begin{aligned}\left\langle H_{0,N} \right\rangle_{\mathrm{bulk}} &= \langle\phi\rangle^2 N + O(1)\,, \\ \left\langle H_{0,N}^2 \right\rangle_{\mathrm{bulk}} &= \langle\phi\rangle^4 N^2 + O(N)\,,\end{aligned} \tag{34}$$

such that

$$R_H = O(1/N) \tag{35}$$

and hence, it vanishes in the limit $N \to \infty$. This implies that the Jensen gap also vanishes in this limit and

$$\Phi(\overline{\tau}_{(I)}) = \left\langle \exp\left(-\frac{\lambda\langle\phi\rangle^2}{\phi_0^2}\right)\right\rangle_0 . \tag{36}$$

Hence, the probability density function of $\overline{\tau}_{(I)}$ obeys

$$\begin{aligned} P(\overline{\tau}_{(I)}) &= \left\langle \delta\left(\overline{\tau}_{(I)} - \frac{\mathrm{e}^{\beta^2\sigma^2/4}}{\phi_0^2}\right)\right\rangle_0 \\ &= \frac{1}{\sqrt{2\pi\,\beta^2\sigma^2}\left(\overline{\tau}_{(I)}\right)^{3/4}} \exp\left(-\frac{\beta^2\sigma^2}{32} - \frac{\ln^2\left(\overline{\tau}_{(I)}\right)}{2\beta^2\sigma^2}\right), \quad 0 \leqslant \overline{\tau}_{(I)} < \infty . \end{aligned} \tag{37}$$

One can straightforwardly check that the first two moments of this function coincide with those defined in equation (24).

The corresponding probability density function of the resistance in the Model II can be calculated using essentially the same kind of arguments. In doing so, we find

$$\begin{aligned} P(\overline{\tau}_{(II)}) &= \left\langle \delta\left(\overline{\tau}_{(II)} - \frac{\mathrm{e}^{\beta^2\sigma^2/4}}{\phi_0\phi_1}\right)\right\rangle_{x=0,1} \\ &= \frac{1}{\sqrt{\pi\,\beta^2\sigma^2}\left(\overline{\tau}_{(II)}\right)^{1/2}} \exp\left(-\frac{\beta^2\sigma^2}{16} - \frac{\ln^2\left(\overline{\tau}_{(II)}\right)}{\beta^2\sigma^2}\right), \quad 0 \leqslant \overline{\tau}_{(II)} < \infty . \end{aligned} \tag{38}$$

It is easy to find that the first two moments of the latter probability density function are given precisely by equation (25). Note, as well, that the probability density functions in equations (37) and (38) have the form of the log-normal distribution as the parental form in equation (5), and differ from it (and between themselves) only in the pre-exponential algebraic dependence on the reduced resistance and by the normalizations.

Lastly, for the Model III the probability density function of the variable $\overline{\tau}_{(III)} = \tau_N^{(III)}/N$ is calculated very straightforwardly. Using equation (6), we find the log-normal distribution of the form

$$\begin{aligned} P(\overline{\tau}_{(III)}) &= \sqrt{\frac{8}{\pi\,\beta^2\sigma^2}} \int_0^1 \frac{\mathrm{d}\phi}{\phi}\,\delta\left(\overline{\tau}_{(III)} - \frac{1}{\phi^2}\right) \exp\left(-\frac{2}{\beta^2\sigma^2}\ln^2(\phi)\right) \\ &= \sqrt{\frac{2}{\pi\,\beta^2\sigma^2}}\,\frac{1}{\overline{\tau}_{(III)}} \exp\left(-\frac{\ln^2\left(\overline{\tau}_{(III)}\right)}{2\beta^2\sigma^2}\right), \quad 1 \leqslant \overline{\tau}_{(III)} < \infty . \end{aligned} \tag{39}$$

Figure 3 illustrates the probability density functions given in equations (37)–(39), along with numerically constructed histograms for the random variable $\overline{\tau}$. The comparison shows an excellent agreement between our analytical predictions and the numerical results.

We close this subsection with the following three remarks:

– The resistances in the Models I and II are not self-averaging in the limit $N \to \infty$, while the resistance in the Model III is not self-averaging for any N. The resistances exhibit significant fluctuations with the relative variances becoming very large when $\beta\sigma$ is large.

– The lack of self-averaging is solely due to fluctuations of the on-site potentials at the site $x = 0$ (for Models I and III) and at the sites $x = 0, 1$ (for Model II). The contributions of the sites in the bulk of the chain are self-averaging for Models I and II, and is constant, i.e., non-fluctuating for the Model III.

– Given the lack of self-averaging of the resistances, it is instructive to consider their typical behavior which should be observed for most of realizations of sequences of U_x and can be accessed by calculating the averaged logarithm of $\overline{\tau}$. Using the expressions (37) and (38), we determine this property to get the following super-Arrhenius function of the temperature for the Models I and II:

$$\overline{\tau}_{\mathrm{typ}}^{(\mathrm{I\ and\ II})} = \exp\left(\left\langle \ln(\overline{\tau}^{(\mathrm{I\ and\ II})})\right\rangle\right) = \exp\left(\frac{\beta^2\sigma^2}{4}\right). \tag{40}$$

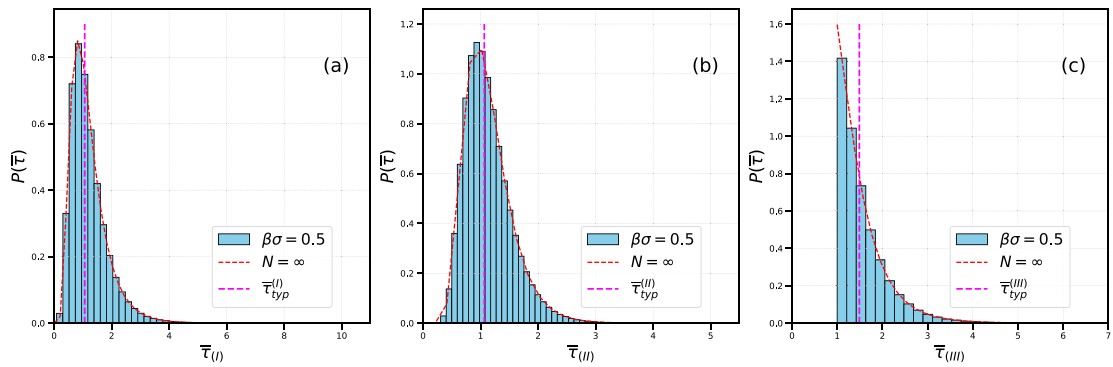

Figure 3. The probability density functions of the reduced resistance $\overline{\tau}$ for the Models I (panel (a)), II (panel (b)) and III (panel (c)). The histograms present the results of a numerical analysis of the random variable $\overline{\tau}$. The enveloping dashed (red) curve depicts our analytical predictions in equations (37)–(39), respectively. Vertical dashed lines indicate the typical values of $\overline{\tau}$ (see equations (40) and (41)).

Unexpectedly, the typical value of $\overline{\tau}$ is the *same* for both Models, despite the fact that their moments grow with $\beta\sigma$ at different rates. The typical value is smaller than the averaged ones, which signifies that the averaged values are supported by some atypical realizations of sequences of the on-site potentials.

Concurrently, for the Model III we find

$$\overline{\tau}^{(III)}_{\rm typ} = \exp\left(\left\langle \ln(\overline{\tau}^{(III)})\right\rangle\right) = \exp\left(\sqrt{\frac{2}{\pi}}\beta\sigma\right). \tag{41}$$

Surprisingly, the typical resistance of a finite chain in the Gaussian random trap model exhibits the Arrhenius dependence on the temperature, in striking contrast to the behavior observed in Models I and II. The typical values of $\overline{\tau}$ are indicated in figure 3 by vertical dashed lines. We observe that for the Models I and II the values of $\overline{\tau}_{\rm typ}$ appear very close to the most probable values of this variable, while for the Model III it is also close to the left edge of the support at which the probability density function attains its maximal value.

3.3. Probability currents

Consider equations (21) and conveniently rewrite them in terms of the reduced random variables $\overline{\tau}$:

$$j^{(I)}_N = \left(\frac{W_0 c_0}{N}\right)\frac{1}{\overline{\tau}_{(I)}}, \quad j^{(II)}_N = \left(\frac{c_0}{2\delta t N}\right)\frac{1}{\overline{\tau}_{(II)}}, \quad j^{(III)}_N = \left(\frac{W_0 c_0}{N}\right)\frac{1}{\overline{\tau}_{(III)}}, \tag{42}$$

where the terms in the brackets can be identified as currents in the absence of disorder. We find next from the expressions (37)–(39) that the large-N asymptotic behavior of the moments of the currents in Models I and II is given explicitly by

$$\begin{aligned}\left\langle \left(j^{(I)}_N\right)^q\right\rangle &= \left(\frac{W_0 c_0}{N}\right)^q \mathrm{e}^{q(2q-1)\beta^2\sigma^2/4},\\ \left\langle \left(j^{(II)}_N\right)^q\right\rangle &= \left(\frac{c_0}{2\delta t N}\right)^q \mathrm{e}^{q(q-1)\beta^2\sigma^2/4},\end{aligned} \tag{43}$$

while for the Model III the exact result, valid for all N, follows

$$\left\langle \left(j^{(III)}_N\right)^q\right\rangle = \left(\frac{W_0 c_0}{N}\right)^q \mathrm{e}^{q^2\beta^2\sigma^2/2}\mathrm{erfc}(q\beta\sigma/\sqrt{2}), \tag{44}$$

where $\mathrm{erfc}(x)$ is the complementary error function. From the above expressions we readily find that the relative variances of the currents obey

$$\begin{aligned}R_{j^{(I)}} &= \exp\left(\beta^2\sigma^2\right) - 1,\\ R_{j^{(II)}} &= \exp\left(\beta^2\sigma^2/2\right) - 1,\\ R_{j^{(III)}} &= \frac{\mathrm{erfc}(\sqrt{2}\,\beta\sigma)}{\mathrm{erfc}^2(\beta\sigma/\sqrt{2})}\exp\left(\beta^2\sigma^2\right) - 1,\end{aligned} \tag{45}$$

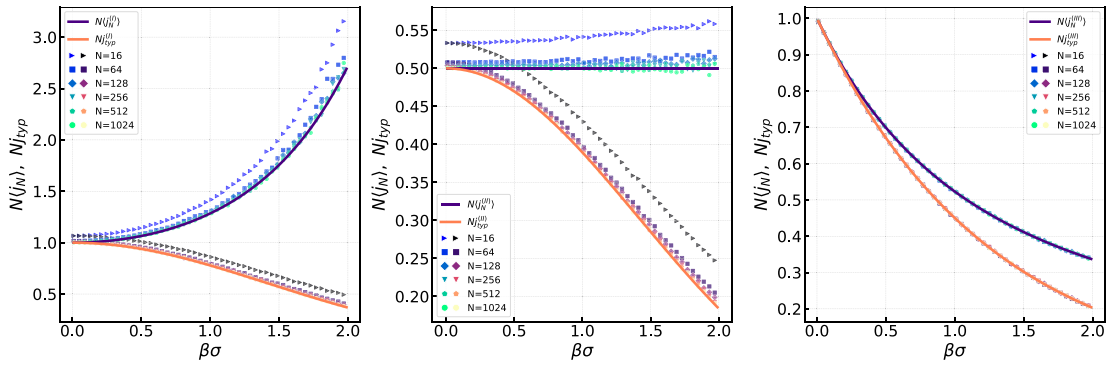

Figure 4. The disorder-averaged versus typical currents (multiplied by N) through a finite interval with N sites for the Models I (left panel), II (middle panel) and III (right panel). The black solid curves depict our analytical predictions for the averaged currents in equations (43) and (44) (with $q = 1$). The red solid curves depict the typical currents in equations (47) and (48). Symbols present the results of a numerical averaging of j_N in equations (42) and the results for an exponentiated averaged $\ln j_N$ (see the inset).

which implies that the currents, likewise the resistances, are not self-averaging in all three Models. Moreover, the corresponding relative variances of the current are monotonically increasing functions of the parameter $\beta\sigma$.

Upon a closer look on the expressions (43) and (44) we notice that the disorder-average currents in the three Models under study exhibit distinctly different behavior as functions of $\beta\sigma$ (see figure 4): in the Model I the disorder-averaged current $\left\langle j_N^{(I)} \right\rangle$ is a monotonically *increasing* function of $\beta\sigma$. This is apparently not very counter-intuitive at the first glance. Indeed, one can imagine such realizations of disorder in which, upon an increase of $\beta\sigma$, we increase the magnitude of random forces which push the particle to move along the chain towards the site $x = N$. Concurrently, the disorder-averaged current in the Model II is *independent* of disorder and has precisely the form of the standard Fickian result for the current in a homogeneous system. This means that evidently in the Model II some very particular, anomalous realizations of disorder control the value of the disorder-averaged current. A similar behavior has been observed previously in [59] for a somewhat different model. On the contrary, in Model III the current is a monotonically *decreasing* function of $\beta\sigma$. In the leading order in the limit $\beta\sigma \to \infty$ the disorder-averaged current in the Gaussian random trap model exhibits a power-law dependence on disorder of the form

$$\left\langle j_N^{(III)} \right\rangle \simeq \left(\frac{W_0 c_0}{N} \right) \sqrt{\frac{2}{\pi}} \frac{1}{\beta\sigma}. \tag{46}$$

In fact, this is again not a counter-intuitive behavior. Indeed, increasing the value of $\beta\sigma$ we increase the depths of traps such that the retention times become larger.

It is important also to compare the behavior of averaged properties against the typical behavior, which should be observed for a majority of realizations of disorder. The typical behavior of the currents can be accessed by merely noticing that, up to the prefactors, in each Model $\ln j_N = -\ln \tau_N$, and by using then our equations (40) and (41). We find that for the Models I and II the typical behavior follows universally

$$j_{\text{typ}}^{(\text{I and II})} = \exp\left(\left\langle \ln j_N^{(\text{I and II})} \right\rangle \right) \sim \mathrm{e}^{-\beta^2\sigma^2/4}, \tag{47}$$

i.e., the typical current in these two Models is characterized by the same *decreasing*, super-Arrhenius function of disorder and the temperature and therefore, is much smaller than the averaged currents in equations (43). Such a strong 'reduction' of the current is apparently due to the fact that in typical realizations of disorder a particle will always get localized between two sites at which sufficiently large forces point in the opposite directions. Further on, we find that in the Model III the typical current obeys

$$j_{\text{typ}}^{(III)} = \exp\left(\left\langle \ln j_N^{(III)} \right\rangle \right) \sim \exp\left(-\sqrt{\frac{2}{\pi}} \beta\sigma \right), \tag{48}$$

i.e., is an exponential Arrhenius function of $\beta\sigma$, in place of the power-law dependence predicted in equation (46). The typical current in this Model also appears to be much smaller than the averaged one.

Expressions (47) and (48) highlight a significant difference between the typical and averaged behavior showing that actually in all scenarios the averaged behavior is supported by atypical realizations of disorder. Behavior of the typical currents is confronted against the one of the averaged currents in figure 4, which substantiates the above discussion.

3.4. Sample-to-sample fluctuations of the resistances and currents

On example of Model I we discuss the behavior of yet another characteristic property which highlights the role of sample-to-sample fluctuations showing how *disproportionally* different, or conversely, similar can be the values of resistances (or currents) observed in two different samples. Following [76, 77], we consider two finite chains of the same length N with two different realizations of the sequences of the on-site potentials U_x. We assume next that the values of the reduced resistances defined in equation (31) are $\overline{\tau}_1$ and $\overline{\tau}_2$, respectively, and the corresponding values of the currents are j_1 and j_2. For brevity, we skip the subscript (I) in what follows as well as the subscript N. Then, we construct a random variable

$$\omega = \frac{\overline{\tau}_1}{\overline{\tau}_1 + \overline{\tau}_2} = \frac{j_2}{j_1 + j_2}, \tag{49}$$

which defines a relative contribution of either of the resistances (currents) to their sum. We seek next the probability density function $P(\omega)$ of this random variable with the support on $(0,1)$. Note that because the probability density functions of the resistances have very similar forms (see equations (37)–(39)), we do not expect any significant difference of the behavior of $P(\omega)$ for the three models under study and therefore, constrain our analysis for the Model I only.

Clearly, the first moment of this random variable $\langle\omega\rangle = 1/2$, by symmetry, but this result can be meaningful or misleading depending on the shape of $P(\omega)$. If $P(\omega)$ is unimodal and centered at $\omega = 1/2$, this will signify that it is most likely that $\overline{\tau}_1 \approx \overline{\tau}_2$ and sample-to-sample fluctuations are not very important. If, on the contrary, $P(\omega)$ is bimodal and has a minimum at $\omega = 1/2$, this will imply that most likely $\overline{\tau}_1$ and $\overline{\tau}_2$ are disproportionally different, despite the fact that averaged value of ω is equal to $1/2$.

In order to calculate $P(\omega)$ we consider first its moment-generating function

$$\begin{aligned}\Phi_\omega &= \left\langle \exp\left(-\lambda\omega\right) \right\rangle \\ &= \int_0^\infty \mathrm{d}\overline{\tau}_1 \int_0^\infty \mathrm{d}\overline{\tau}_2 \exp\left(-\lambda \frac{\overline{\tau}_1}{\overline{\tau}_1 + \overline{\tau}_2}\right) P(\overline{\tau}_1)\, P(\overline{\tau}_2)\,,\end{aligned} \tag{50}$$

where $P(\overline{\tau})$ is defined in equation (37). Changing formally the integration variable $\overline{\tau}_1 \to \omega$, equation (49), we have

$$\Phi_\omega = \int_0^1 \frac{\mathrm{d}\omega}{(1-\omega)^2}\, \mathrm{e}^{-\lambda\omega} \int_0^\infty \overline{\tau}_2\, \mathrm{d}\overline{\tau}_2\, P(\overline{\tau}_2)\, P\left(\frac{\omega}{1-\omega}\,\overline{\tau}_2\right), \tag{51}$$

from which we can readily read of the desired probability density function

$$\begin{aligned}P(\omega) &= \frac{1}{(1-\omega)^2} \int_0^\infty \overline{\tau}_2\, \mathrm{d}\overline{\tau}_2\, P(\overline{\tau}_2)\, P\left(\frac{\omega}{1-\omega}\,\overline{\tau}_2\right) \\ &= \frac{1}{2\sqrt{\pi\,\beta^2\sigma^2}\,\omega(1-\omega)} \exp\left(-\frac{\ln^2\left(\omega/(1-\omega)\right)}{4\beta^2\sigma^2}\right).\end{aligned} \tag{52}$$

This probability density function is depicted in figure 5 for three values of the parameter $\beta\sigma$. We observe that for a relatively small disorder, i.e., for $\beta\sigma = 0.1$, $P(\omega)$ is unimodal and centered at $\omega = 1/2$. This signifies that for a small disorder it is indeed most likely that the values of resistances (or currents) observed in two randomly chosen samples are very close to each other. Upon an increase of $\beta\sigma$, for $\beta\sigma = 1$, we encounter a different behavior when the central part of $P(\omega)$ becomes flat and $\omega = 1/2$ is no longer the most probable value. In this situation, (almost) any relation between the two resistance becomes equally probable. Increasing $\beta\sigma$ further, we have that already for $\beta\sigma = 1.2$ the probability density function becomes bimodal with two maxima close to $\omega = 0$ and $\omega = 1$. Here, $\omega = 1/2$ corresponds not to the most probable but to the *least* probable value. This signifies that the resistance (or currents) observed in two sample are most likely disproportionally different and sample-to-sample fluctuations are very significant.

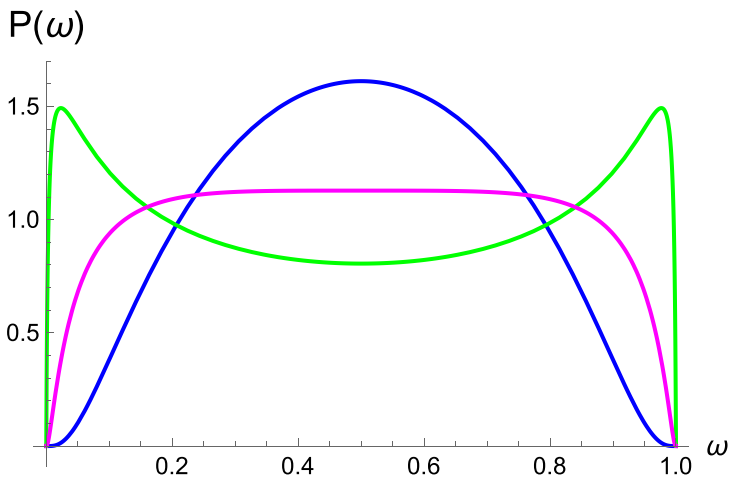

Figure 5. Sample-to-sample fluctuations. Probability density function $P(\omega)$ in equation (52) as function of ω for $\beta\sigma = 0.1$ (blue curve), $\beta\sigma = 1$ (magenta curve) and $\beta\sigma = 1.2$ (green curve).

4. The realization-dependent splitting probability

Consider a one-dimensional chain composed of $N+1$ sites labeled $x = 0, 1, \ldots, N$. Suppose that the particle starts at site $x = x_0$ and performs a CTRW with site-dependent transition rates $W_{x,x+1}$ (to the right, $x \to x+1$) and $W_{x,x-1}$ (to the left, $x \to x-1$). The sites $x = 0$ and $x = N$ at the boundaries are absorbing, meaning that once the particle reaches either boundary, it remains there forever. We focus here on the so-called *splitting probability* $E_-(x_0)$; that is, the probability that a particle starting from the site x_0 is eventually absorbed at the left boundary $x = 0$ before ever reaching the right boundary $x = N$.

In appendix B we show that the realization-dependent splitting probability admits the following compact representation,

$$E_-(x_0) = \frac{\tau^+_{N-x_0}}{\tau^-_{x_0} + \tau^+_{N-x_0}}, \tag{53}$$

where $\tau^+_{x_0}$ and $\tau^-_{N-x_0}$ are the resistances of the intervals $(0, x_0-1)$ and (x_0+1, N) from the left and from the right of the starting point x_0, respectively. These realization-dependent resistances are defined explicitly by rather lengthy expressions (see equations (B.8)) which we present in appendix B. An analogous expression for the continuous-space system can be found in [45].

As shown in appendix B, the realization-dependent splitting probability for Model III is trivially $E_-(x_0) = 1 - x_0/N$, i.e., it is not a fluctuating property and is the same as in homogeneous systems without disorder [66]. Concurrently, for the Models I and II the splitting probabilities do depend on disorder and for both Models are given by

$$E_-(x_0) = \frac{H_{x_0,N}}{H_{0,N}}, \tag{54}$$

where the function $H_{x_0,N}$ is defined by equation (23) with the first index replaced by x_0. A straightforward analysis shows that in the joint limit $N, x_0 \to \infty$ with the ratio $\alpha = x_0/N$ kept fixed,

$$\frac{1}{N}\sum_{x=0}^{N-1} \phi_x \phi_{x+1} \xrightarrow[N\to\infty]{} \langle \phi \rangle^2, \qquad \frac{1}{N-x_0}\sum_{x=x_0}^{N-1} \phi_x \phi_{x+1} \xrightarrow[N,x_0\to\infty]{} \langle \phi \rangle^2,$$

almost surely. As a consequence, the realization-dependent splitting probability self-averages in this limit and converges to

$$E_-(x_0) \simeq 1 - \frac{x_0}{N}, \tag{55}$$

with vanishing sample-to-sample fluctuations.

In figure 6 we show the splitting probability as a function of the scaled position $\alpha = x_0/N$. The top row (left panel) displays the realization-dependent $E_-(x_0)$ given by equation (53), evaluated for a single

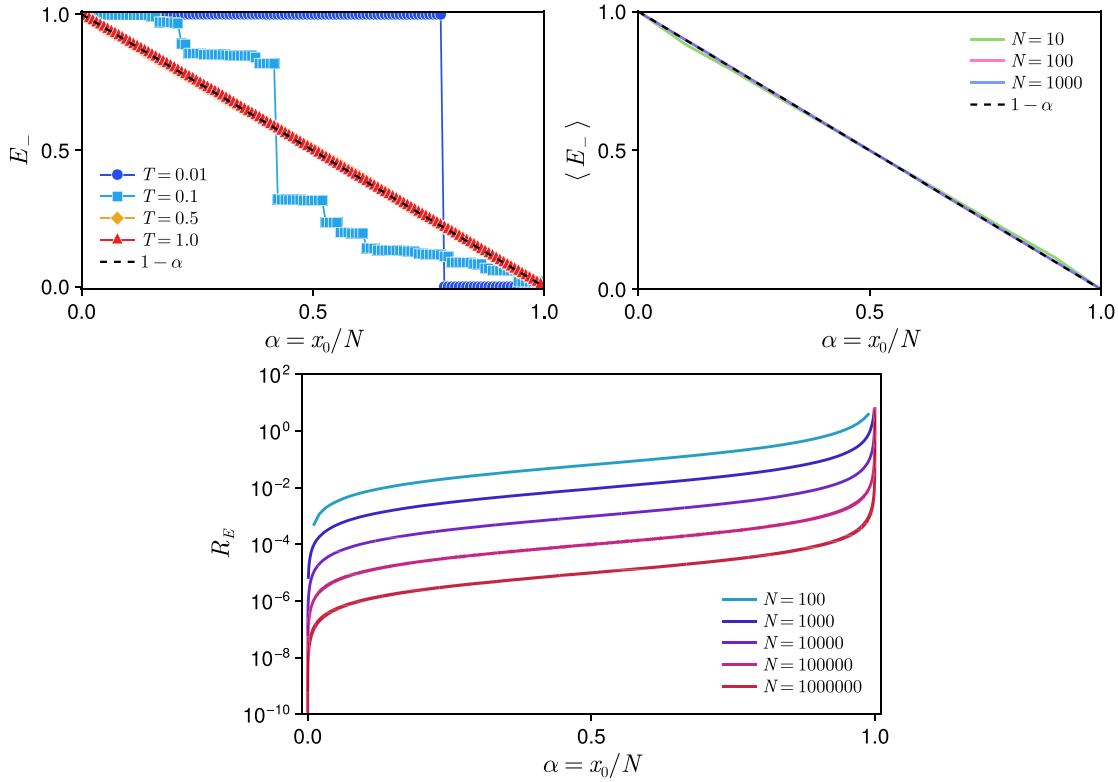

Figure 6. The splitting probability $E_-(x_0)$ as function of $\alpha = x_0/N$. Top row: The splitting probability in equation (54) for a given realization of disorder on a chain with $N = 10^5$ sites for different temperatures (left panel). Numerically-evaluated first moment of the splitting probability for several values of N at fixed inverse temperature $\beta = 10$ (right panel). In both panels the dashed line depicts the analytical prediction in equation (55). Bottom row: Relative variance $R_E = \mathrm{Var}(E_-(x_0))/\langle E_-(x_0)\rangle^2$ for $\beta = 2$ and several values of N.

randomly generated disorder realization on a chain of 10^5 sites, at several temperatures. At the lowest temperature ($T = 0.01$), the sum $H_{0,N}$ is entirely dominated by its largest term. As a result, the splitting probability takes the form of a step function: $E_-(x_0) = 1$ up to a critical realization-dependent value of α, beyond which it drops abruptly to zero. When the temperature is increased by an order of magnitude, subdominant contributions to $H_{0,N}$ become relevant. Consequently, $E_-(x_0)$ develops a descending staircase-like structure as a function of α, with each plateau corresponding to dominance of different terms in the sum. Upon further increase of the temperature, the realization-dependent fluctuations are progressively smoothed out. In this regime, the realization-dependent splitting probability becomes nearly indistinguishable from that of a homogeneous system, recovering the linear behavior $E_-(x_0) = 1 - \alpha$ [66]. Next, the top-right panel of figure 6 shows the numerically evaluated disorder-averaged splitting probability for several values of N at a fixed temperature. We find that all curves are nearly indistinguishable from the asymptotic prediction in equation (55), indicating that size-dependent corrections remain very small, even at the relatively low temperature $T = 0.1$. Lastly, the bottom row of figure 6 displays the relative variance of the realization-dependent splitting probability as a function of $\alpha = x_0/N$ for several values of N (see inset), at a fixed inverse temperature $\beta = 2$. Away from the boundaries $\alpha = 0$ and $\alpha = 1$, where E_- equals 1 and 0, respectively, and hence $R_E \equiv 0$, the relative variance is nonzero for finite N but decreases systematically as N increases. In the limit $N \to \infty$, R_E vanishes, indicating that the splitting probability becomes self-averaging. We note finally that the exact expressions for the splitting probability derived in this section can alternatively be obtained by applying the general formalism for random walks with spatially inhomogeneous hopping probabilities detailed in [78].

5. The realization-dependent mean first-passage times

Consider a finite chain with $N+1$ sites x, $x = 0, 1, \ldots, N$, in which the site $x = N$ is the 'target'. A particle starts from the site at the left extremity of the chain, i.e., from $x = 0$, performs a random walk in a continuous-time between the nearest-neighboring sites of the chain and reaches for the first time the right extremity at some random time instant, which is called the

first-passage time to N. The mean first-passage time T_N, with the averaging being performed over all possible realizations of the random walk process for a fixed realization of the transition rates $W_{x,x\pm1}$, is an important characteristic property of random transport processes which has been amply analyzed in the past (see, e.g., [48–50, 65–69]). A comprehensive and systematic derivation of the expressions for the mean first-passage time discussed below can also be obtained from the general formal solutions presented in [78].

Here we follow an early work [70] in which an explicit expression for T_N has been derived for the continuous-time and discrete-space master equation for the general form of the transition rates. Adapting this result to our notations, one has

$$T_N = \frac{\eta_N}{\theta_N}\sum_{j=0}^{N-1}\theta_j - \sum_{j=0}^{N-1}\eta_j\,, \tag{56}$$

where

$$\begin{aligned}
&\theta_0 = 1\,, \quad \theta_j = \frac{W_{0,1}W_{1,2}W_{2,3}\ldots W_{j-1,j}}{W_{1,0}W_{2,1}W_{3,2}\ldots W_{j,j-1}}\,,\\
&\eta_0 = 0\,, \quad \eta_j = \frac{1}{W_{j,j-1}}\left[1 + \frac{W_{j-1,j}}{W_{j-1,j-2}} + \frac{W_{j-1,j}W_{j-2,j-1}}{W_{j-1,j-2}W_{j-2,j-3}} + \ldots + \frac{W_{j-1,j}W_{j-2,j-1}W_{j-3,j-2}\ldots W_{1,2}}{W_{j-1,j-2}W_{j-2,j-3}W_{j-3,j-4}\ldots W_{1,0}}\right].
\end{aligned} \tag{57}$$

For the Model I the rates are defined in equation (7), while for the Model II we have $W_{x,y} = p_{x,y}/\delta t$ with the transition probabilities $p_{x,y}$ defined in equation (11).

For the Model I we find

$$\theta_{j\geqslant 0} = \frac{\phi_0^2}{\phi_j^2}\,, \quad \eta_{j\geqslant 1} = \frac{H_{0,j}}{W_0\phi_j^2} = \frac{1}{W_0\phi_j^2}\sum_{x=0}^{j-1}\phi_x\phi_{x+1}\,, \eta_0 = 0\,, \tag{58}$$

such that the realization-dependent mean first-passage time is given by

$$T_N^{(I)} = \frac{1}{W_0}\sum_{j=0}^{N-1}\frac{1}{\phi_j^2}\sum_{x=j}^{N-1}\phi_x\phi_{x+1}\,. \tag{59}$$

Correspondingly, the first two moments of $T_N^{(I)}$ are given by

$$\begin{aligned}
\left\langle T_N^{(I)}\right\rangle &= \frac{N^2}{2W_0}\left\langle\frac{1}{\phi^2}\right\rangle\langle\phi\rangle^2 + O(N) = \frac{N^2}{2W_0}\mathrm{e}^{3\beta^2\sigma^2/4} + O(N)\,,\\
\left\langle\left(T_N^{(I)}\right)^2\right\rangle &= \frac{N^4}{4W_0^2}\left\langle\frac{1}{\phi^2}\right\rangle^2\langle\phi\rangle^4 + O\left(N^3\right) = \frac{N^4}{4W_0^2}\mathrm{e}^{3\beta^2\sigma^2/2} + O\left(N^3\right)\,.
\end{aligned} \tag{60}$$

Turning to the Model II and noting that the transition probabilities depend on the on-site potentials at both neighboring sites, we have to define $U_{x=-1}$ and $U_{x=N+1}$. For simplicity, we suppose that we have impermeable barriers at these two sites such that $U_{x=-1} = U_{x=N+1} = \infty$ and hence, $\phi_{-1} = \phi_{N+1} = \infty$. Then, after some algebra we have

$$\begin{aligned}
&\eta_0 = 0\,, \quad \eta_{j\geqslant 1} = \delta t\left(\frac{1}{\phi_{j-1}\phi_j} + \frac{1}{\phi_j\phi_{j+1}}\right)H_{0,j} = \delta t\left(\frac{1}{\phi_{j-1}\phi_j} + \frac{1}{\phi_j\phi_{j+1}}\right)\sum_{x=0}^{j-1}\phi_x\phi_{x+1}\,,\\
&\theta_j = \phi_0\phi_1\left(\frac{1}{\phi_{j-1}\phi_j} + \frac{1}{\phi_j\phi_{j+1}}\right).
\end{aligned} \tag{61}$$

Inserting the above equations into equation (56), we get the following expression for the realization-dependent mean first-passage time

$$T_N^{(II)} = \delta t\sum_{j=0}^{N-1}\left(\frac{1}{\phi_{j-1}\phi_j} + \frac{1}{\phi_j\phi_{j+1}}\right)\sum_{x=j}^{N-1}\phi_x\phi_{x+1}\,. \tag{62}$$

Averaging the expression (62) we find

$$\begin{aligned}\left\langle T_N^{(II)}\right\rangle &= \frac{(2\delta t)N^2}{2}\left\langle\frac{1}{\phi}\right\rangle^2\langle\phi\rangle^2 + O(N) = \frac{(2\delta t)N^2}{2}\mathrm{e}^{\beta^2\sigma^2/2} + O(N)\,,\\ \left\langle\left(T_N^{(II)}\right)^2\right\rangle &= \frac{(2\delta t)^2N^4}{4W_0^2}\left\langle\frac{1}{\phi}\right\rangle^4\langle\phi\rangle^4 + O\left(N^3\right) = \frac{(2\delta t)^2N^4}{4}\mathrm{e}^{\beta^2\sigma^2} + O\left(N^3\right).\end{aligned} \tag{63}$$

Lastly, we turn to the Model III for which the rates obey equation (20) and hence,

$$\theta_{j\geqslant 0} = \frac{\phi_0^2}{\phi_j^2}\,,\quad \eta_{j\geqslant 0} = \frac{j}{W_0\phi_j^2}\,, \tag{64}$$

such that the realization-dependent mean first-passage time attains a very compact form

$$T_N^{(III)} = \frac{1}{W_0}\sum_{j=0}^{N-1}\frac{(N-j)}{\phi_j^2}\,. \tag{65}$$

Respectively, the first and second moments of $T_N^{(III)}$ evaluated by averaging the above expression with the probability density function in equation (6) are given by

$$\begin{aligned}\left\langle T_N^{(III)}\right\rangle &= \frac{N(N+1)}{2W_0}\mathrm{e}^{\beta^2\sigma^2/2}\left(1+\mathrm{erf}\left(\beta\sigma/\sqrt{2}\right)\right),\\ \left\langle\left(T_N^{(III)}\right)^2\right\rangle &= \frac{(N-1)N(N+1)(3N+2)}{12W_0^2}\mathrm{e}^{\beta^2\sigma^2}\left(1+\mathrm{erf}\left(\beta\sigma/\sqrt{2}\right)\right)^2\\ &\quad+\frac{N(2N^2+3N+1)}{6W_0^2}\mathrm{e}^{2\beta^2\sigma^2}\left(1+\mathrm{erf}\left(\sqrt{2}\,\beta\sigma\right)\right).\end{aligned} \tag{66}$$

It is then straightforward to conclude that for all three models the relative variance of the realization-dependent mean first-passage times obeys

$$R_T = O(1/N)\,, \tag{67}$$

which means that these properties are self-averaging in the limit $N\to\infty$. However, as we have already remarked, this just shows the trend that fluctuations become relatively less important the farther the target is located away from the starting point. For all practically important applications N is essentially finite and fluctuations are therefore important. In particular, in the physically relevant problem of protein target search on DNA, sequence-dependent binding energies generate a random energy landscape with experimentally inferred disorder strengths typically in the range $\beta\sigma\sim 1-5$ [42]. Moreover, the distances explored during individual sliding events are usually of the order of $N\sim 10-10^3$ base pairs. Consequently, the non-self-averaging effects predicted by our theory are not merely of theoretical interest but may have observable consequences for protein search kinetics in heterogeneous genomic environments.

In figure 7 we present numerically-evaluated probability density functions of the realization-dependent reduced mean first-passage times $\overline{T} = T_N/N^2$ for several values of the distance N to the target and three models under study. We observe that, in full accord with our prediction in equation (67), the probability density functions become narrower and more sharply peaked at the disorder-averaged values of the mean first-passage times, the larger N is.

6. The realization-dependent diffusion coefficient

Most of existing analyses of the effective diffusion coefficient of particles diffusing in a random Gaussian potential focus on one-dimensional, periodic, *continuous-space* systems with period L (see, e.g., [10, 51]). These studies often build upon the well-known expression for the effective diffusion coefficient in a periodic continuum with an arbitrary potential U_x, originally derived by Lifson and Jackson [71] (see also [72])

$$D_L = \frac{D_0L^2}{\int_0^L \mathrm{d}x\mathrm{e}^{\beta U_x}\int_0^L \mathrm{d}y\mathrm{e}^{-\beta U_y}}\,, \tag{68}$$

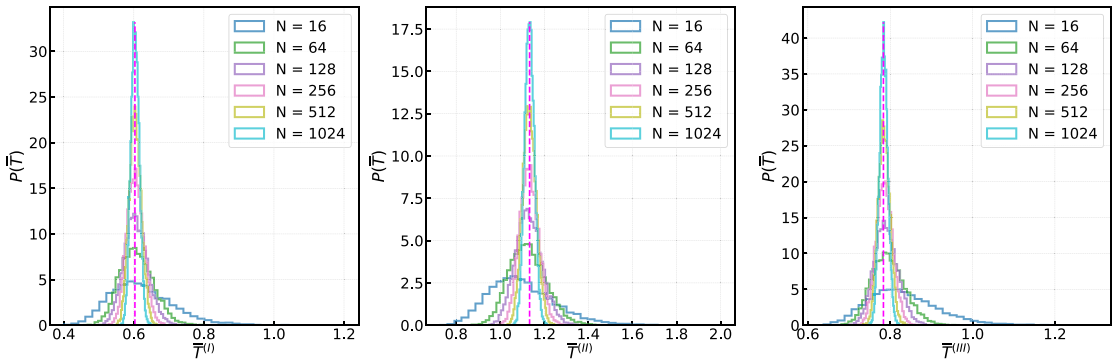

Figure 7. Numerically-evaluated normalized probability density functions of the reduced mean first-passage times $\overline{T} = T_N/N^2$ for the Models I (left panel), II (middle panel) and III (right panel) and different values of the distance N to the target (see the insets). Vertical dashed lines indicate positions the disorder-averaged mean first passage times.

where D_0 is the diffusion coefficient in absence of the external potential U_x. Averaging the above expression and going to the limit $L \to \infty$, in order to describe the behavior in infinitely large systems, several notable results have been obtained. In particular, it was shown that for a Gaussian random potential with the probability density function in equation (2) one has [8] (see also [51] for a review)

$$\left\langle D_L \right\rangle = D_0 \, \mathrm{e}^{-\beta^2\sigma^2} . \tag{69}$$

This result demonstrates that the diffusion coefficient decreases in the presence of a Gaussian random potential—a physically intuitive outcome. Remarkably, the reduction factor takes the form of a simple exponential function of $\beta^2\sigma^2$, exhibiting therefore a pronounced super-Arrhenius dependence on temperature.

In this section we seek for the analogues of the result in equation (68) for the random walks on *discrete* periodic chains with N sites and also for different types of dynamics, as defined in our Models I, II and III. To this end, we will make use of Derrida's general, though rather intricate, expression for the effective diffusion coefficient D_N, valid for an arbitrary set of transition rates [4]. In appendix C we present details of the derivation of D_N for the three models under study. Then, we will determine the moments of D_N, discuss their dependence on $\beta\sigma$ and on this basis will demonstrate that the realization-dependent diffusion coefficient is self-averaging in the limit $N \to \infty$, regardless of the dynamical scenario.

6.1. Model I: random force-like model

In appendix C we show that for such a model the Derrida's formula [4] reduces to the following expression

$$D_N = \frac{W_0 N^2}{\sum_{x=1}^{N} \mathrm{e}^{-\beta U_x} \sum_{y=1}^{N} \mathrm{e}^{\frac{\beta}{2}(U_y + U_{y+1})}} = \frac{W_0 N^2}{\sum_{x=1}^{N} \phi_x^{-2} \sum_{y=1}^{N} \phi_y \phi_{y+1}} , U_{N+x} = U_x . \tag{70}$$

The above expression does not have an apparent symmetry $U_x \to -U_x$, unlike the original Lifson–Jackson formula (68), but converges to it if we rewrite equation (70) for an arbitrary inter-site spacing a and then turn to the continuous-space limit $a \to 0$.

We introduce next an auxiliary function

$$\Theta_N^{(I)}(\lambda_1, \lambda_2) = \left\langle \exp\left(-\Psi_N^{(I)}(\lambda_1, \lambda_2) \right) \right\rangle , \tag{71}$$

where

$$\Psi_N^{(I)}(\lambda_1, \lambda_2) = \frac{\lambda_1}{N} \sum_{x=1}^{N} \phi_x^{-2} + \frac{\lambda_2}{N} \sum_{x=1}^{N} \phi_x \phi_{x+1} . \tag{72}$$

One may readily notice that the moments of the realization-dependent diffusion coefficient in equation (70) can be evaluated by a mere integration of $\Theta_N^{(I)}(\lambda_1, \lambda_2)$,

$$\left\langle D_N^q \right\rangle = \frac{W_0^q}{\Gamma^2(q)} \int_0^\infty \int_0^\infty \mathrm{d}\lambda_1 \, \mathrm{d}\lambda_2 (\lambda_1 \lambda_2)^{q-1} \Theta_N^{(I)}(\lambda_1, \lambda_2) . \tag{73}$$

We turn to the limit $N \to \infty$ and consider the first two moments of the functional $\Psi_N^{(I)}(\lambda_1, \lambda_2)$. These moments can be evaluated very straightforwardly to give

$$\begin{aligned} \left\langle \Psi_N^{(I)}(\lambda_1,\lambda_2) \right\rangle &= \lambda_1 \left\langle \frac{1}{\phi^2} \right\rangle + \lambda_2 \langle \phi \rangle^2 \\ \left\langle \left(\Psi_N^{(I)}(\lambda_1,\lambda_2) \right)^2 \right\rangle &= \lambda_1^2 \left\langle \frac{1}{\phi^2} \right\rangle^2 + \lambda_2^2 \langle \phi \rangle^4 + 2\lambda_1\lambda_2 \left\langle \frac{1}{\phi^2} \right\rangle \langle \phi \rangle^2 + O(1/N) . \end{aligned} \tag{74}$$

Since the leading terms in the second equation can be expressed as the square of the right-hand-side of the first equation, it follows that the function $\Psi_N^{(I)}(\lambda_1, \lambda_2)$ is self-averaging in the limit $N \to \infty$, such that

$$\Theta_{N\to\infty}^{(I)}(\lambda_1,\lambda_2) = \exp\left(-\lambda_1 \left\langle \frac{1}{\phi^2} \right\rangle - \lambda_2 \langle \phi \rangle^2 \right) . \tag{75}$$

Consequently, the moments of D_N in an infinite system obey

$$\left\langle D_{N\to\infty}^q \right\rangle = \frac{W_0^q}{\langle 1/\phi^2 \rangle^q \langle \phi \rangle^{2q}} = W_0^q \exp\left(-3q\beta^2\sigma^2/4 \right) . \tag{76}$$

The effective diffusion coefficient is therefore self-averaging in the limit $N \to \infty$.

6.2. Model II: random walks with randomized stepping-times

In appendix C we show that for this model the realization-dependent diffusion coefficient obeys the following symmetric form

$$\begin{aligned} D_N &= \frac{N^2}{2\delta t \left(\sum_{x=1}^N \mathrm{e}^{-\frac{\beta}{2}(U_x+U_{x+1})} \right) \left(\sum_{y=1}^N \mathrm{e}^{\frac{\beta}{2}(U_y+U_{y+1})} \right)} \\ &= \frac{N^2}{2\delta t \sum_{x=1}^N \frac{1}{\phi_x\phi_{x+1}} \sum_{y=1}^N \phi_y\phi_{y+1}} , U_x = U_{x+N} , \end{aligned} \tag{77}$$

which resembles the Lifson–Jackson formula but with a rather non-evident 'discretization' scheme. This compact form preserves the symmetry $U_x \to -U_x$ and reduces to the expression (68) upon the passage to the continuous-space limit.

As above, we introduce an auxiliary function

$$\Theta_N^{(II)}(\lambda_1,\lambda_2) = \left\langle \exp\left(-\Psi_N^{(II)}(\lambda_1,\lambda_2) \right) \right\rangle , \tag{78}$$

where $\Psi_N^{(II)}(\lambda_1, \lambda_2)$ is now given by

$$\Psi_N^{(I)}(\lambda_1,\lambda_2) = \frac{\lambda_1}{N} \sum_{x=1}^N \frac{1}{\phi_x\phi_{x+1}} + \frac{\lambda_2}{N} \sum_{x=1}^N \phi_x\phi_{x+1} . \tag{79}$$

Once this function is determined, the moments of D_N of an arbitrary (not necessarily integer) order q are then simply given by the integral

$$\left\langle D_N^q \right\rangle = \frac{1}{(2\delta t)^q \Gamma^2(q)} \int_0^\infty \int_0^\infty \mathrm{d}\lambda_1 \mathrm{d}\lambda_2 (\lambda_1\lambda_2)^{q-1} \Theta_N^{(II)}(\lambda_1,\lambda_2) . \tag{80}$$

Further on, we consider the first two moments of the functional $\Psi_N^{(II)}(\lambda_1, \lambda_2)$ to get

$$\begin{aligned} \left\langle \Psi_N^{(II)}(\lambda_1,\lambda_2) \right\rangle &= \lambda_1 \left\langle \frac{1}{\phi} \right\rangle^2 + \lambda_2 \langle \phi \rangle^2 \\ \left\langle \left(\Psi_N^{(II)}(\lambda_1,\lambda_2) \right)^2 \right\rangle &= \lambda_1^2 \left\langle \frac{1}{\phi} \right\rangle^4 + \lambda_2^2 \langle \phi \rangle^4 + 2\lambda_1\lambda_2 \left\langle \frac{1}{\phi} \right\rangle^2 \langle \phi \rangle^2 + O(1/N) . \end{aligned} \tag{81}$$

Again, we observe that the leading terms in the equation in the second line are just the full square of the right-hand-side of the equation in the first line, which signifies that the functional $\Psi_N^{(II)}(\lambda_1,\lambda_2)$ is self-averaging in the limit $N\to\infty$. As a consequence,

$$\Theta^{(I)}_{N\to\infty}(\lambda_1,\lambda_2)=\exp\left(-\lambda_1\left\langle\frac{1}{\phi}\right\rangle^2-\lambda_2\langle\phi\rangle^2\right), \tag{82}$$

such that the moments of the effective diffusion coefficient in an infinite system read

$$\left\langle D^q_{N\to\infty}\right\rangle=\frac{1}{(2\delta t)^q\langle 1/\phi\rangle^{2q}\langle\phi\rangle^{2q}}=\frac{1}{(2\delta t)^q}\exp\left(-q\beta^2\sigma^2/2\right). \tag{83}$$

The effective diffusion coefficient is evidently self-averaging in the limit $N\to\infty$.

We close these two subsections with the following two remarks:

– Neither the expression (76) nor the expression (83) reproduce *exactly* the result in equation (69), obtained in [8] for the continuous-space expression for the effective diffusion coefficient in equation (68): both dynamical scenarios yield indeed a simple exponential, super-Arrhenius dependence on $\beta^2\sigma^2$ but predict somewhat different values of the numerical factors.

– At the same time, a 'direct' discretization of the continuous-space Lifson–Jackson formula (68) gives

$$D_N=\frac{D_0N^2}{\sum_{x=1}^N \mathrm{e}^{\beta U_x}\sum_{y=1}^N \mathrm{e}^{-\beta U_y}}=\frac{D_0N^2}{\sum_{x=1}^N \phi_x^2\sum_{y=1}^N \phi_y^{-2}}. \tag{84}$$

Using the above arguments about the self-averaging in the limit $N\to\infty$, we find that

$$\left\langle D^q_{N\to\infty}\right\rangle=D_0^q\exp\left(-q\beta^2\sigma^2\right), \tag{85}$$

which gives precisely the expression (69) for $q=1$. On the other hand, we could not find (and doubt if they exist) the transition rates $W_{x,x\pm1}$ for the microscopic stochastic dynamics on the discrete lattice which will give exactly the form in equation (84).

6.3. Model III: Gaussian random trap model

We show in appendix C that within this dynamical scenario the realization-dependent effective diffusion coefficient attains a particularly simple form:

$$D_N=\frac{W_0N}{\sum_{x=1}^N \mathrm{e}^{-\beta U_x}}=\frac{W_0N}{\sum_{x=1}^N \phi_x^{-2}}. \tag{86}$$

As above, our next step consists in introducing an auxiliary function

$$\Theta^{(III)}(\lambda)=\lim_{N\to\infty}\left\langle\exp\left(-\frac{\lambda}{N}\sum_{x=1}^N\phi_x^{-2}\right)\right\rangle, \tag{87}$$

such that the moments of $D_{N\to\infty}$ can be obtained by performing the integral

$$\left\langle D^q_{N\to\infty}\right\rangle=\frac{W_0^q}{\Gamma(q)}\int_0^\infty\lambda^{q-1}\,\mathrm{d}\lambda\,\Theta^{(III)}(\lambda) \tag{88}$$

The auxiliary function $\Theta^{(III)}(\lambda)$ can be calculated very straightforwardly to give

$$\begin{aligned}\Theta^{(III)}(\lambda)&=\lim_{N\to\infty}\left[\int_0^1\mathrm{d}\phi\,\mathrm{e}^{-\lambda/N\phi^2}P_-(\phi)\right]^N=\lim_{N\to\infty}\left[1-\int_0^1\mathrm{d}\phi\,\left(1-\mathrm{e}^{-\lambda/N\phi^2}\right)P_-(\phi)\right]^N\\&=\exp\left(-\lambda\int_0^1\frac{\mathrm{d}\phi}{\phi^2}P_-(\phi)\right)=\exp\left(-\lambda\mathrm{e}^{\beta^2\sigma^2}\left(1+\mathrm{erf}\left(\beta\sigma/\sqrt{2}\right)\right)\right).\end{aligned} \tag{89}$$

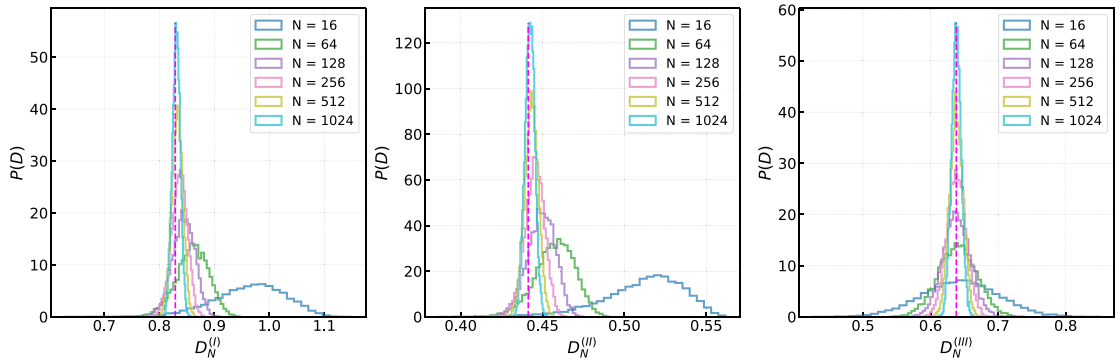

Figure 8. Numerically-evaluated normalized probability density functions of the effective diffusion coefficients for the Models I (left panel), II (middle panel) and III (right panel) for different values of N ranging from $N = 16$ to $N = 1024$ (see the insets). Vertical dashed lines indicate the limiting ($N \to \infty$) values of the disorder-averaged diffusion coefficients (see equations (76), (83) and (90) with $q = 1$).

Inserting the latter expression into equation (88) and performing the integral, we find

$$\left\langle D^q_{N\to\infty} \right\rangle = \frac{W_0^q}{\left(1+\mathrm{erf}\left(\beta\sigma/\sqrt{2}\right)\right)^q} \mathrm{e}^{-q\beta^2\sigma^2/2}. \tag{90}$$

One can readily check directly that also for the Model III the diffusion coefficient is self-averaging in the limit $N \to \infty$.

Finally, for all three models, we numerically compute the probability density functions of the diffusion coefficients for several values of N. As shown in figure 8, the distributions become progressively narrower and increasingly concentrated around the disorder-averaged diffusion coefficients (indicated by the vertical dashed lines) as N grows.

7. Conclusions

In conclusion, we have revisited the long-standing problem of random walks in the presence of a quenched Gaussian random potential, a topic that has attracted considerable attention in the past. Specifically, we analyzed the continuous-time dynamics of a particle performing nearest-neighbor random walks on a one-dimensional lattice, where each site x hosts a quenched random potential U_x that governs the local transition rates. The onsite potentials U_x are assumed to be independent and identically distributed Gaussian random variables.

We have considered three distinct dynamical scenarios, each characterized by a different dependence of the transition rates on the onsite potentials U_x: (i) a random-force-like model, (ii) a CTRW with exponentially distributed waiting times, where the transition probabilities depend on the potentials on neighboring sites, and (iii) a Gaussian random trap model.

For all three scenarios, we analyzed the statistical properties of five realization-dependent random variables: (a) the steady-state probability current through a finite chain with N sites, (b) its reciprocal, representing the resistance of a finite interval with N sites with respect to random transport, (c) the splitting probability—the probability that a particle starting at site x_0 within the interval $(0, N)$ first reaches the left boundary without ever visiting the right boundary, (d) the mean first-passage time across a finite interval of length N, and (e) the diffusion coefficient in a finite periodic chain with N sites.

For all these random variables we have calculated analytically the leading (in the large-N limit) asymptotic behavior of their moments determining the dependence on the strength of disorder and the temperature. We have shown that these moments exhibit an interesting super-Arrhenius dependence on the temperature, which is also quite different depending on the dynamical scenario. Comparing the averaged and the typical behavior we have demonstrated that the moments of the resistance and currents are supported by atypical realizations of disorder.

For intermediate values of N, we have performed numerical analyses, employing exact numerical averaging of the formal expressions that define these properties for a given sequence of U_x values.

Further on, we have addressed a conceptually important question whether these transport properties exhibit self-averaging with respect to different realizations of disorder in the limit $N \to \infty$. Capitalizing

on the derived exact expressions for the moments, we have studied the asymptotic behavior of their relative variances. We have shown that the probability currents through finite chains and the resistances of these chains are not self-averaging in the limit $N \to \infty$. Interestingly enough, such a lack of self-averaging appears to be a boundary effect; namely, it stems from fluctuations of one (or a few) sites close to the boundary, while the contributions coming from the sites in the bulk of chains are self-averaging.

Concurrently, we have shown that the realization-dependent splitting probability and the realization-dependent mean first-passage time to a target placed at distance N away from the starting point are *self-averaging* in the limit $N \to \infty$. Clearly, this result just indicates the trend in the behavior of fluctuations that they become progressively less important the farther is the target away from the starting point. However, for most of practical applications N is essentially finite and our numerical analysis shows that for such N fluctuations are quite significant.

Lastly, we have shown that for all three dynamical scenarios the realization-dependent diffusion coefficient in periodic chains with N sites is self-averaging in the limit $N \to \infty$. This result is very meaningful because it applies to the dynamics in infinite systems. For finite N the diffusion coefficient also exhibits essential sample-to-sample fluctuations.

In summary, our results show that even relatively simple Gaussian disorder can have a substantial impact on transport properties, giving rise to both self-averaging and non-self-averaging regimes. We expect this classification to extend beyond Gaussian disorder to a broad class of models with finite disorder moments, for which standard Central Limit Theorem arguments suggest that the qualitative behavior remains unchanged. In contrast, a much stronger influence of disorder is anticipated in systems with heavy-tailed distributions, such as the random trap model with exponentially distributed trap depths or the Touya-Dean model [9]. In these cases, the relevant realization-dependent quantities may lack finite moments, leading to dynamics dominated by rare events and a much more severe breakdown of self-averaging. The investigation of such strongly anomalous regimes constitutes a natural direction for future work.

Acknowledgements

The authors wish to thank E Agliari, T Akimoto, D S Dean, E Barkai and L A Pastur for helpful discussions. This project has been supported by funding from the 2021 first FIS (Fondo Italiano per la Scienza) funding scheme (FIS783—SMaC—Statistical Mechanics and Complexity University and Research) from Italian MUR (Ministry of University and Research).

Data availability statement

All data that support the findings of this study are included within the article (and any supplementary files).

Appendix A. Realization-dependent probability current

Consider a finite chain in which we fix the value of the probability $P_{x=0} = P(x=0,t) = c_0$ (see equation (16)) at the site $x=0$, and place a perfect sink at the site $x=N$, such that $P_{x=N} = P(x=N,t)=0$. Then, in such a situation the evolution equations (16) become

$$\begin{aligned}
\dot{P}_1 &= -(W_{1,0}+W_{1,2})P_1 + W_{0,1}c_0 + W_{2,1}P_2\,,\\
\dot{P}_2 &= -(W_{2,1}+W_{2,3})P_2 + W_{1,2}P_1 + W_{3,2}P_3\,,\\
\dot{P}_3 &= -(W_{3,2}+W_{3,4})P_3 + W_{2,3}P_2 + W_{4,3}P_4\,,\\
&\cdots\\
\dot{P}_{N-1} &= -(W_{N-1,N-2}+W_{N-1,N})P_{N-1} + W_{N-2,N-1}P_{N-2}\,.
\end{aligned} \tag{A.1}$$

Setting next $\dot{P}_x = 0$ for all x, and solving the resulting linear system of equations recursively, we get for P_{N-1}:

$$P_{N-1} = \frac{W_{0,1}c_0}{W_{N-1,N}\Sigma_N}\,, \tag{A.2}$$

where Σ_N obeys

$$\Sigma_N = 1 + \frac{W_{1,0}}{W_{1,2}} + \frac{W_{1,0}W_{2,1}}{W_{1,2}W_{2,3}} + \frac{W_{1,0}W_{2,1}W_{3,2}}{W_{1,2}W_{2,3}W_{3,4}} + \frac{W_{1,0}W_{2,1}W_{3,2}W_{4,3}}{W_{1,2}W_{2,3}W_{3,4}W_{4,5}} + \ldots + \frac{W_{1,0}W_{2,1}W_{3,2}W_{4,3}\ldots W_{N-2,N-3}}{W_{1,2}W_{2,3}W_{3,4}W_{4,5}\ldots W_{N-2,N-1}} + \frac{W_{1,0}W_{2,1}W_{3,2}W_{4,3}\ldots W_{N-2,N-3}W_{N-1,N-2}}{W_{1,2}W_{2,3}W_{3,4}W_{4,5}\ldots W_{N-2,N-1}W_{N-1,N}}.$$

Respectively, the realization-dependent current to the sink at $x = N$ obeys

$$j_N = W_{N-1,N}P_{N-1} = \frac{W_{0,1}c_0}{\Sigma_N}. \tag{A.3}$$

For the Model I the rates are defined in equations (7), which gives

$$\Sigma_N^{(I)} = \frac{1}{\phi_0\phi_1}\left(\phi_0\phi_1 + \phi_1\phi_2 + \phi_2\phi_3 + \ldots + \phi_{N-1}\phi_N\right). \tag{A.4}$$

Hence, the realization-dependent current to the sink is given by

$$j_N^{(I)} = \frac{\phi_0 W_0 c_0}{\phi_1 \Sigma_N^{(I)}}, \tag{A.5}$$

from which we find the first expression in equation (21).

For the Model II, the rates obey

$$W_{x,x\pm1} = \frac{p_{x,x\pm1}}{\delta t}, \tag{A.6}$$

where the normalized transition probabilities are defined in equation (13). Upon some algebra we find that Σ_N in equation (A.3) for this model is exactly the same as for the Model I, i.e., it obeys equation (A.4). Consequently, the steady-state realization-dependent current to the sink follows

$$j_N^{(II)} = \frac{\phi_{-1}}{(\phi_{-1}+\phi_1)}\frac{c_0}{\delta t \Sigma_N^{(I)}}. \tag{A.7}$$

Supposing, for simplicity, that the potential on the site $x = -1$ is exactly the same as at the site $x = 1$, we get the second expression in equation (21).

For the Model III with the rates given by equation (20), one finds that Σ_N is independent of the depths of the traps and is simply given by

$$\Sigma_N^{(III)} = N, \tag{A.8}$$

i.e., is not fluctuating. Correspondingly, the steady-state current obeys

$$j_N^{(III)} = \frac{W_0 c_0 \phi_0^2}{N}, \tag{A.9}$$

from which we read of the third expression in equation (21).

Appendix B. Realization-dependent splitting probability

In this appendix we derive an explicit expression for the splitting probability E_-. We consider a continuous-time random walk on a finite one-dimensional lattice with sites $x = 0, 1, \ldots, N$, with the transition rates $W_{x,x+1}$ and $W_{x,x-1}$ for jumps from the site x to the neighboring sites $x-1$ and $x+1$. Let $E_-(x_0)$ denote the probability that, starting from site x_0, the random walk visits the left boundary at $x = 0$ before reaching the right boundary at $x = N$.

As shown in [79] the splitting probability $E_-(x)$ (here, the walk is assumed to start at arbitrary point x, excluding $x = 0$ and $x = N$) satisfies the *backward* master equation of the form

$$W_{x,x+1}\left[E_-(x+1) - E_-(x)\right] + W_{x,x-1}\left[E_-(x-1) - E_-(x)\right] = 0, \quad x = 1, \ldots, N-1, \tag{B.1}$$

which is to be solved subject to trivial boundary conditions :

$$E_-(x=0) = 1, \qquad E_-(x=N) = 0. \tag{B.2}$$

Equation (B.1) can be conveniently rewritten in terms of finite differences $\Delta E_-(x) = E_-(x+1) - E_-(x)$,

$$\Delta E_-(x) = \frac{W_{x,x-1}}{W_{x,x+1}}\,\Delta E_-(x-1), \qquad 1 \leqslant x < N. \tag{B.3}$$

and solved recursively to give

$$\Delta E_-(x) = \Delta E_-(0) \prod_{k=1}^{x} \frac{W_{k,k-1}}{W_{k,k+1}}\,. \tag{B.4}$$

The above expression yields the following explicit expression in terms of $E_-(x)$:

$$E_-(x) = 1 + \Delta E_-(0)\Sigma_x\,, \tag{B.5}$$

in which $\Delta E_-(0)$ is as yet an undefined parameter and the sum Σ_x has been introduced in appendix A,

$$\Sigma_x = 1 + \sum_{j=1}^{x-1} \prod_{k=1}^{j} \frac{W_{k,k-1}}{W_{k,k+1}}. \tag{B.6}$$

Lastly, the boundary condition $E_-(N) = 0$ ensures that

$$\Delta E_-(0) = -\frac{1}{\Sigma_N},$$

and hence, the general solution for $x = x_0$ reads

$$E_-(x_0) = 1 - \frac{\Sigma_{x_0}}{\Sigma_N} = \frac{\displaystyle\sum_{j=x_0}^{N-1} \prod_{k=1}^{j} \frac{W_{k,k-1}}{W_{k,k+1}}}{\displaystyle 1 + \sum_{j=1}^{N-1} \prod_{k=1}^{j} \frac{W_{k,k-1}}{W_{k,k+1}}}. \tag{B.7}$$

We note next that the above expression (B.7) can be cast into a compact form in equation (53), where $\tau^-_{x_0}$ and $\tau^+_{N-x_0}$ represent, respectively, the resistances of the intervals $(0, x_0 - 1)$ and $(x_0 + 1, N)$ from the left and from the right of the starting point x_0:

$$\begin{aligned} \tau^-_{x_0} &= \frac{1}{W_{x_0,x_0-1}} \left(1 + \frac{W_{x_0-1,x_0}}{W_{x_0-1,x_0-2}} + \cdots + \frac{W_{x_0-1,x_0} \cdots W_{1,2}}{W_{x_0-1,x_0-2} \cdots W_{1,0}} \right), \\ \tau^+_{N-x_0} &= \frac{1}{W_{x_0,x_0+1}} \left(1 + \frac{W_{x_0+1,x_0}}{W_{x_0+1,x_0+2}} + \cdots + \frac{W_{x_0+1,x_0} \cdots W_{N-1,N-2}}{W_{x_0+1,x_0+2} \cdots W_{N-1,N}} \right). \end{aligned} \tag{B.8}$$

This is done by simply noticing that equation (B.7) can be formally rewritten as

$$\begin{aligned} E_-(x_0) &= \frac{\displaystyle\sum_{j=x_0}^{N-1} \prod_{k=1}^{j} \frac{W_{k,k-1}}{W_{k,k+1}}}{\displaystyle 1 + \sum_{j=1}^{N-1} \prod_{k=1}^{j} \frac{W_{k,k-1}}{W_{k,k+1}}} \\ &= \frac{\dfrac{W_{1,0} \ldots W_{x_0 x_0 - 1}}{W_{1,2} \ldots W_{x_0,x_0+1}} + \cdots + \dfrac{W_{1,0} \ldots W_{N-1,N-2}}{W_{1,2} \ldots W_{N-1,N}}}{1 + \dfrac{W_{1,0}}{W_{1,2}} + \cdots + \dfrac{W_{1,0} \ldots W_{x_0,x_0-1}}{W_{1,2} \ldots W_{x_0,x_0+1}} + \cdots + \dfrac{W_{1,0} \ldots W_{N-1,N-2}}{W_{1,2} \ldots W_{N-1,N}}} \\ &= \left(1 + \frac{W_{x_0+1,x_0}}{W_{x_0+1,x_0+2}} + \cdots + \frac{W_{x_0+1,x_0} \ldots W_{N-1,N-2}}{W_{x_0+1,x_0+2} \ldots W_{N-1,N}} \right) \\ &\quad \Big/ \left(\frac{W_{1,2} \ldots W_{x_0,x_0+1}}{W_{1,0} \ldots W_{x_0,x_0-1}} + \cdots + \frac{W_{x_0,x_0+1}}{W_{x_0,x_0-1}} + 1 + \frac{W_{x_0+1,x_0}}{W_{x_0+1,x_0+2}} + \cdots + \frac{W_{x_0+1,x_0} \ldots W_{N-1,N-2}}{W_{x_0+1,x_0+2} \ldots W_{N-1,N}} \right) \end{aligned} \tag{B.9}$$

and then factoring out the common product $W_{1,0}\cdots W_{x_0,x_0-1}/W_{1,2}\cdots W_{x_0,x_0+1}$ from both numerator and denominator.

Consider next the model-specific forms of the splitting probability $E_-(x_0)$.

Model I. Using the general expressions derived in appendix A, we have that the resistances of the intervals from the left and from the right from the starting site x_0 attain the following forms:

$$\begin{aligned}\tau^-_{x_0} &= \frac{1}{\phi_x^2}\left(\phi_{x_0}\phi_{x_0-1}+\phi_{x_0-1}\phi_{x_0-2}+\cdots+\phi_1\phi_0\right),\\ \tau^+_{N-x_0} &= \frac{1}{\phi_{x_0}^2}\left(\phi_{x_0}\phi_{x_0+1}+\phi_{x_0+1}\phi_{x_0+2}+\cdots+\phi_{N-1}\phi_N\right),\end{aligned} \tag{B.10}$$

where ϕ_x is defined in the main text. This gives for the Model I the following expression

$$E_-^{(I)}(x_0) = \frac{\phi_{x_0}\phi_{x_0+1}+\phi_{x_0+1}\phi_{x_0+2}+\cdots+\phi_{N-1}\phi_N}{\phi_0\phi_1+\cdots+\phi_{N-1}\phi_N} = \frac{H_{x_0,N}}{H_{0,N}}. \tag{B.11}$$

Model II. In this case the resistances admit the following form

$$\begin{aligned}\tau^-_{x_0} &= \frac{\phi_{x_0+1}+\phi_{x_0-1}}{\phi_{x_0+1}\phi_{x_0}\phi_{x_0-1}}\left(\phi_{x_0}\phi_{x_0-1}+\phi_{x_0-1}\phi_{x_0-2}+\cdots+\phi_1\phi_0\right),\\ \tau^+_{N-x_0} &= \frac{\phi_{x_0-1}+\phi_{x_0+1}}{\phi_{x_0-1}\phi_{x_0}\phi_{x_0+1}}\left(\phi_{x_0}\phi_{x_0+1}+\phi_{x_0+1}\phi_{x_0+2}+\cdots+\phi_{N-1}\phi_N\right).\end{aligned} \tag{B.12}$$

Noticing that the multipliers $(\phi_{x_0-1}+\phi_{x_0+1})/\phi_{x_0-1}\phi_{x_0}\phi_{x_0+1}$ cancel each other, we find that also for the Model II the splitting probability $E_-^{(II)}(x_0)$ obeys equation (B.11).

Model III. For the random trap model the transition rates are symmetric and hence,

$$\tau^-_{x_0} = \frac{x_0}{\phi_{x_0}^2}, \quad \tau^+_{N-x_0} = \frac{N-x_0}{\phi_{x_0}^2}. \tag{B.13}$$

Consequently, we find that $E_-^{(III)}(x_0)$ is independent of disorder (i.e., it is not a fluctuating property) and obeys

$$E_-^{(III)}(x_0) = 1-\frac{x_0}{N}. \tag{B.14}$$

Appendix C. Realization-dependent diffusion coefficient

In this appendix, we present the derivation of our expressions for the realization-dependent diffusion coefficients in the Models I, II and III (see equations (70), (77) and (86)) taking advantage of the general result due to Derrida [4] for random walks in periodic one-dimensional systems with arbitrary fixed transition rates.

Derrida's result. For completeness, we present below the Derrida's general result for the realization-dependent D_N for random walks evolving in a continuous time on a finite periodic chain with N sites with arbitrary fixed transition rates $W_{x,x\pm1}$. As shown by Derrida [4], the realization-dependent diffusion coefficient in such a setting has the following form

$$D_N = \frac{1}{\left(\sum_{n=1}^N r_n\right)^2}\left(V\sum_{n=1}^N u_n\sum_{i=1}^N \mathrm{i}\, r_{n+i} + N\sum_{n=1}^N W_{n,n+1}\,u_n\,r_n\right) - V\frac{N+2}{2}, \tag{C.1}$$

where the functions u_n and r_n are defined as

$$u_n = \frac{1}{W_{n,n+1}}\left[1+\sum_{i=1}^{N-1}\prod_{j=1}^{i}\left(\frac{W_{n-j+1,n-j}}{W_{n-j,n-j+1}}\right)\right], \tag{C.2}$$

$$r_n = \frac{1}{W_{n,n+1}}\left[1+\sum_{i=1}^{N-1}\prod_{j=1}^{i}\left(\frac{W_{n+j,n+j-1}}{W_{n+j,n+j+1}}\right)\right], \tag{C.3}$$

while V is the mean (averaged over thermal noise) velocity for a given realization of disorder :

$$V = \frac{N}{\sum_{n=1}^{N} r_n}\left[1 - \prod_{n=1}^{N}\left(\frac{W_{n+1,n}}{W_{n,n+1}}\right)\right]. \tag{C.4}$$

Model I. For the Model I the transition rates are defined in equation (7). Using this definition, we find

$$\prod_{n=1}^{N}\frac{W_{n+1,n}}{W_{n,n+1}} = \prod_{n=1}^{N}\frac{\phi_{n+1}^2}{\phi_n^2} = 1, \tag{C.5}$$

which implies that the mean realization-dependent velocity for this model is exactly equal to zero, as it should.

We proceed to compute the quantities needed for the evaluation of the diffusion coefficient. The first is r_n, which becomes

$$\begin{aligned} r_n &= \frac{1}{W_0}\frac{\phi_{n+1}}{\phi_n}\left[1 + \sum_{i=1}^{N-1}\prod_{j=1}^{i}\left(\frac{\phi_{n+j}}{\phi_{n+j-1}}\cdot\frac{\phi_{n+j+1}}{\phi_{n+j}}\right)\right] \\ &= \frac{1}{W_0}\frac{\phi_{n+1}}{\phi_n}\left[1 + \frac{\phi_{n+2}}{\phi_n} + \frac{\phi_{n+2}\phi_{n+3}}{\phi_n\phi_{n+1}} + \cdots + \frac{\phi_{n+N-1}\phi_{n+N}}{\phi_n\phi_{n+1}}\right] \\ &= \frac{1}{W_0}\frac{1}{\phi_n^2}\left(\phi_n\phi_{n+1} + \phi_{n+1}\phi_{n+2} + \cdots + \phi_{n+N-1}\phi_{n+N}\right) = \frac{1}{W_0}\frac{1}{\phi_n^2}H_{0,N}, \end{aligned} \tag{C.6}$$

where $H_{0,N}$ is given in equation (23). Further on, from equation (C.6) we have that

$$\sum_{n=1}^{N} r_n = \frac{1}{W_0}H_{0,N}\sum_{n=1}^{N}\frac{1}{\phi_n^2} = \frac{1}{W_0}H_{0,N}K_{0,N}, \tag{C.7}$$

where we used the shortening

$$K_{n,n+N} \equiv \sum_{i=0}^{N-1}\frac{1}{\phi_{n+i}^2} = K_{0,N}. \tag{C.8}$$

Next, we calculate u_n by substituting the rates into equation (C.2) which gives

$$\begin{aligned} u_n &= \frac{1}{W_0}\frac{\phi_{n+1}}{\phi_n}\left[1 + \sum_{i=1}^{N-1}\prod_{j=1}^{i}\left(\frac{\phi_{n-j+1}^2}{\phi_{n-j}^2}\right)\right] \\ &= \frac{1}{W_0}\frac{\phi_{n+1}}{\phi_n}\left[1 + \frac{\phi_n^2}{\phi_{n-1}^2} + \frac{\phi_n^2\phi_{n-1}^2}{\phi_{n-1}^2\phi_{n-2}^2} + \cdots + \frac{\phi_n^2\cdots\phi_{n-N+2}^2}{\phi_{n-1}^2\cdots\phi_{n-N+1}^2}\right] \\ &= \frac{1}{W_0}\phi_n\phi_{n+1}\sum_{i=0}^{N-1}\frac{1}{\phi_{n-i}^2} = \frac{1}{W_0}\phi_n\phi_{n+1}K_{0,N}. \end{aligned} \tag{C.9}$$

Lastly, upon some algebra, we find that

$$\begin{aligned} \sum_{n=1}^{N} W_{n,n+1}u_n r_n &= \sum_{n=1}^{N}\frac{\phi_n}{\phi_{n+1}}\cdot\phi_n\phi_{n+1}K_{0,N}\cdot\frac{1}{W_0}\frac{1}{\phi_n^2}H_{0,N} \\ &= \sum_{n=1}^{N}K_{0,N}\cdot\frac{1}{W_0}H_{0,N} = \frac{N}{W_0}K_{0,N}H_{0,N}. \end{aligned} \tag{C.10}$$

Combining all the above results, we obtain the following expression for the realization-dependent diffusion coefficient in the Model I:

$$\begin{aligned} D_N^{(I)} &= \frac{N}{\left(\sum_{n=1}^{N} r_n\right)^2}\left(\sum_{n=1}^{N} W_{n,n+1}u_n r_n\right) = \frac{N}{\left(\frac{1}{W_0}H_{0,N}K_{0,N}\right)^2}\cdot\frac{N}{W_0}K_{0,N}H_{0,N} \\ &= \frac{W_0 N^2}{H_{0,N}K_{0,N}}, \end{aligned} \tag{C.11}$$

which is exactly the expression (70) in the main text.

Model II. In this dynamical scenario with randomized stepping-times, the transition rates $W_{x,x\pm1} = p_{x,x\pm1}/\delta t$, where $p_{x,x\pm1}$ are the transition probabilities of an auxiliary random process that obey equations (11) and (13). Firstly, we notice that

$$\prod_{k=1}^{N}\frac{p_{k,k-1}}{p_{k,k+1}} = \prod_{k=1}^{N}\frac{\phi_{k+1}}{\phi_{k-1}+\phi_{k+1}}\cdot\frac{\phi_{k-1}+\phi_{k+1}}{\phi_{k-1}} = \prod_{k=1}^{N}\frac{\phi_{k+1}}{\phi_{k-1}} = 1\,, \tag{C.12}$$

which signifies that the mean realization-dependent velocity is exactly equal to zero, as it should.

Next, we evaluate r_n:

$$\begin{aligned} r_n &= \frac{1}{p_{n,n+1}}\left(1+\sum_{i=1}^{N-1}\prod_{j=1}^{i}\frac{p_{n+j,n+j-1}}{p_{n+j,n+j+1}}\right) = \frac{\phi_{n-1}+\phi_{n+1}}{\phi_{n-1}}\left(1+\sum_{i=1}^{N-1}\prod_{j=1}^{i}\frac{\phi_{n+j+1}}{\phi_{n+j-1}}\right) \\ &= \frac{\phi_{n-1}+\phi_{n+1}}{\phi_{n-1}\phi_n\phi_{n+1}}H_{n,n+N} = \left(\frac{1}{\phi_n\phi_{n+1}}+\frac{1}{\phi_n\phi_{n-1}}\right)H_{0,N}. \end{aligned} \tag{C.13}$$

Summing the above expression over n we find:

$$\sum_{n=1}^{N} r_n = \sum_{n=1}^{N}\left(\frac{1}{\phi_n\phi_{n+1}}+\frac{1}{\phi_n\phi_{n-1}}\right)H_{0,N} = 2H_{0,N}Q_{0,N}\,, \tag{C.14}$$

with

$$Q_{n,n+N} \equiv \sum_{i=0}^{N-1}\frac{1}{\phi_{n+i}\phi_{n+1+i}} = Q_{0,N}\,. \tag{C.15}$$

Next, for u_n we find

$$\begin{aligned} u_n &= \frac{1}{p_{n,n+1}}\left(1+\sum_{i=1}^{N-1}\prod_{j=1}^{i}\frac{p_{n+1-j,n-j}}{p_{n-j,n-j+1}}\right) \\ &= \frac{\phi_{n-1}+\phi_{n+1}}{\phi_{n-1}}\left(1+\sum_{i=1}^{N-1}\prod_{j=1}^{i}\frac{\phi_{n-j+2}}{\phi_{n-j}+\phi_{n-j+2}}\cdot\frac{\phi_{n-j-1}+\phi_{n-j+1}}{\phi_{n-j-1}}\right) \\ &= 2\phi_n\phi_{n+1}Q_{0,N}. \end{aligned} \tag{C.16}$$

Lastly, we evaluate the sum

$$\begin{aligned} \sum_{n=1}^{N} p_{n,n+1}u_n r_n &= \sum_{n=1}^{N}\frac{\phi_{n-1}}{\phi_{n-1}+\phi_{n+1}}\cdot 2\phi_n\phi_{n+1}Q_{0,N}\cdot\frac{\phi_{n-1}+\phi_{n+1}}{\phi_{n-1}\phi_n\phi_{n+1}}H_{0,N} \\ &= 2NH_{0,N}Q_{0,N}. \end{aligned} \tag{C.17}$$

Combining the above expressions, we find the following compact result for the realization-dependent diffusion coefficient in the Model II :

$$\begin{aligned} D_N^{(II)} &= \frac{N}{\left(\sum_{n=1}^{N} r_n\right)^2}\sum_{n=1}^{N} p_{n,n+1}u_n r_n = \frac{N}{(2H_{0,N}Q_{0,N})^2}\cdot 2NH_{0,N}Q_{0,N} \\ &= \frac{N^2}{2H_{0,N}Q_{0,N}}\,, \end{aligned} \tag{C.18}$$

which is our equation (77) in the main text.

Model III. In the Gaussian random trap model the transition rates obey equation (20). It is straightforward to verify that the product

$$\prod_{n=1}^{N}\frac{W_{n+1,n}}{W_{n,n+1}} = \prod_{n=1}^{N}\frac{\phi_{n+1}^2}{\phi_n^2} = 1\,, \tag{C.19}$$

which implies that the mean velocity for this model is also equal to zero for any realization of disorder.

Next, for the quantity r_n we find

$$r_n = \frac{1}{W_0}\frac{1}{\phi_n^2}\left[1+\sum_{i=1}^{N-1}\prod_{j=1}^{i}\left(\frac{\phi_{n+j}^2}{\phi_{n+j}^2}\right)\right] = \frac{1}{W_0}\frac{N}{\phi_n^2}, \tag{C.20}$$

and consequently,

$$\sum_{n=1}^{N} r_n = \sum_{n=1}^{N}\frac{1}{W_0}\frac{N}{\phi_n^2} = \frac{N}{W_0}K_{0,N}. \tag{C.21}$$

Next, we have that u_n obeys

$$\begin{aligned} u_n &= \frac{1}{W_0}\frac{1}{\phi_n^2}\left[1+\sum_{i=1}^{N-1}\prod_{j=1}^{i}\frac{\phi_{n-j+1}^2}{\phi_{n-j}^2}\right] \\ &= \frac{1}{W_0}\frac{1}{\phi_n^2}\left[1+\frac{\phi_n^2}{\phi_{n-1}^2}+\frac{\phi_n^2\phi_{n-1}^2}{\phi_{n-1}^2\phi_{n-2}^2}+\cdots+\frac{\phi_n^2\cdots\phi_{n-N+2}^2}{\phi_{n-1}^2\cdots\phi_{n-N+1}^2}\right] \\ &= \frac{1}{W_0}\sum_{i=0}^{N-1}\frac{1}{\phi_{n-i}^2} = \frac{1}{W_0}K_{0,N}. \end{aligned} \tag{C.22}$$

Lastly, we get

$$\begin{aligned} \sum_{n=1}^{N} W_{n,n+1}u_n r_n &= \sum_{n=1}^{N} W_0\phi_n^2\cdot\frac{1}{W_0}K_{0,N}\cdot\frac{1}{W_0}\frac{N}{\phi_n^2} \\ &= \frac{N^2}{W_0}K_{0,N}. \end{aligned} \tag{C.23}$$

Combining all the above expressions we find from equation (C.1) the following expression for the realization-dependent diffusion coefficient in the Model III:

$$\begin{aligned} D_N^{(III)} &= \frac{N}{\left(\sum_{n=1}^{N} r_n\right)^2}\left(\sum_{n=1}^{N} W_{n,n+1}u_n r_n\right) \\ &= \frac{NW_0^2}{N^2K_{0,N}^2}\cdot\frac{N^2}{W_0}K_{0,N} = \frac{W_0 N}{K_{0,N}}, \end{aligned} \tag{C.24}$$

which is the expression (86) in the main text.

ORCID iDs

Silvio Kalaj 0009-0004-0416-0981
Luca Peliti 0000-0002-1371-100X

References

[1] Anderson P W 1958 Absence of diffusion in certain random lattices *Phys. Rev.* **109** 1492
[2] Derrida B and Luck J M 1983 Diffusion on a random lattice: weak-disorder expansion in arbitrary dimension *Phys. Rev. B* **28** 7183
[3] Luck J M 1983 Diffusion in a random medium: a renormalization group approach *Nucl. Phys. B* **225** 169
[4] Derrida B 1983 Velocity and diffusion constant of a periodic one-dimensional hopping model *J. Stat. Phys.* **31** 433
[5] Fisher D S 1984 Random walks in random environments *Phys. Rev. A* **30** 960
[6] Durrett R 1986 Multidimensional random walks in random environments with subclassical limiting behavior *Commun. Math. Phys.* **104** 87–102
[7] Bramson M and Durrett R 1988 Random walk in random environment: a counterexample? *Commun. Math. Phys.* **119** 199
[8] Zwanzig R 1988 Diffusion in a rough potential *Proc. Natl Acad. Sci. USA* **85** 2029
[9] Touya C and Dean D S 2007 Dynamical transition for a particle in a squared Gaussian potential *J. Phys. A: Math. Theor.* **40** 919
[10] Dean D S, Drummond I T and Horgan R R 1997 Continuum Derrida approach to drift and diffusivity in random media *J. Phys. A: Math. Gen.* **30** 385
[11] Sinai Y G 1982 The limiting behavior of a one-dimensional random walk in a random medium *Theor. Prob. Appl.* **27** 256
[12] Derrida B and Pomeau Y 1982 Classical diffusion on a random chain *Phys. Rev. Lett.* **48** 627
[13] Marinari E, Parisi G, Ruelle D and Windey P 1983 Random walk in a random environment and $1/f$ noise *Phys. Rev. Lett.* **50** 1223

[14] Marinari E, Parisi G, Ruelle D and Windey P 1983 On the interpretation of $1/f$ noise *Commun. Math. Phys.* **89** 1–12
[15] Fisher D S, Friedan D, Qiu Z, Shenker S J and Shenker S H 1985 Random walks in two-dimensional random environments with constrained drift forces *Phys. Rev. A* **31** 3841
[16] Kesten H 1986 The limit distribution of Sinai's random walk in random environment *Physica A* **138** 299
[17] Doussal P L, Cugliandolo L F and Peliti L 1997 Dynamics of particles and manifolds in random force fields *Europhys. Lett.* **39** 111
[18] Comtet A and Dean D S 1998 Exact results on Sinai's diffusion *J. Phys. A: Math. Gen.* **31** 8595
[19] Oshanin G, Mogutov A and Moreau M 1993 Steady flux in a continuous-space Sinai chain *J. Stat. Phys.* **73** 379
[20] Monthus C and Comtet A 1994 On the flux distribution in a one dimensional disordered system *J. Phys. I France* **4** 635
[21] Oshanin G, Rosso A and Schehr G 2013 Anomalous fluctuations of currents in sinai-type random chains with strongly correlated disorder *Phys. Rev. Lett.* **110** 100602
[22] Dean D S, Gupta S, Oshanin G, Rosso A and Schehr G 2014 Diffusion in periodic, correlated random forcing landscapes *J. Phys. A: Math. Theor.* **47** 372001
[23] Bouchaud J P 1992 Weak ergodicity breaking and aging in disordered systems *J. Phys. I France* **2** 1705
[24] Cugliandolo L and Doussal P L 1996 Large time off-equilibrium dynamics of a particle diffusing in a random potential *Phys. Rev. E* **53** 1525
[25] Monthus C and Bouchaud J-P 1996 Models of traps and glass phenomenology *J. Phys. A: Math. Gen.* **29** 3847
[26] Bertin E and Bouchaud J-P 2002 Dynamical ultrametricity in the critical trap model *J. Phys. A: Math. Gen.* **35** 3039
[27] Bertin E M and Bouchaud J-P 2003 Sub-diffusion and localization in the one-dimensional trap model *Phys. Rev. E* **67** 026128
[28] Krüsemann H, Godec A and Metzler R 2014 First-passage statistics for aging diffusion in systems with annealed and quenched disorder *Phys. Rev. E* **89** 040101(R)
[29] Krüsemann H, Godec A and Metzler R 2015 Ageing first passage time density in continuous time random walks and quenched energy landscapes *J. Phys. A: Math. Theor.* **48** 285001
[30] Godec A and Metzler R 2015 Optimization and universality of Brownian search in a basic model of quenched heterogeneous media *Phys. Rev. E* **91** 052134
[31] Akimoto T, Barkai E and Saito K 2016 universal fluctuations of single-particle diffusivity in quenched environment *Phys. Rev. Lett.* **117** 180602
[32] Akimoto T, Barkai E and Saito K 2018 Non-self averaging and ergodicity in quenched trap model with finite system size *Phys. Rev. E* **97** 052143
[33] Park S, Durang X, Metzler R and Jeon J-H Fickian yet non-Gaussian diffusion in an annealed heterogeneous environment (arXiv:2503.15366)
[34] Matheron G and de Marsily G 1980 Is transport in porous medium always diffusive: a counterexample *Water Resour. Res.* **16** 901
[35] Oshanin G and Blumen A 1994 Rouse chain dynamics in layered random flows *Phys. Rev. E* **49** 4185
[36] Wiese K J and Doussal P L 1999 Polymers and manifolds in static random flows: a renormalization group study *Nucl. Phys. B* **552** 529
[37] Bouchaud J-P, Georges A, Koplik J, Provata A and Redner S 1990 Superdiffusion in random velocity fields *Phys. Rev. Lett.* **64** 2503
[38] Mejia-Monasterio C, Nechaev S, Oshanin G and Vasilyev O 2020 Tracer diffusion on a crowded random Manhattan lattice *New J. Phys.* **22** 033024
[39] Kafri Y, Lubensky D K and Nelson D R 2004 Dynamics of molecular motors and polymer translocation with sequence heterogeneity *Biophys. J.* **86** 3373
[40] Kafri Y and Nelson D R 2005 Sequence heterogeneity and the dynamics of molecular motors *J. Phys.: Condens. Matter* **17** S3871
[41] Kafri Y, Lubensky D K and Nelson D R 2005 Dynamics of molecular motors with finite processivity on heterogeneous tracks *Phys. Rev. E* **71** 041906
[42] Slutsky M, Kardar M and Mirny L A 2004 Diffusion in correlated random potentials, with applications to DNA *Phys. Rev. E* **69** 061903
[43] Hwa T, Marinari E, Sneppen K and Tang L-h 2003 Localization of denaturation bubbles in random DNA sequences Proc *Natl Acad. Sci. USA* **100** 4411
[44] de Gennes P G 1975 Brownian motion of a classical particle through potential barriers. Application to the helix-coil transitions of heteropolymers *J. Stat. Phys.* **12** 463
[45] Oshanin G and Redner S 2009 Helix or coil? Fate of a melting heteropolymer *Eur. Phys. Lett.* **85** 10008
[46] Alexander S, Bernasconi J, Schneider W R and Orbach R 1981 Excitation dynamics in random one-dimensional systems *Rev. Mod. Phys.* **53** 175
[47] Peliti L 1984 Self-avoiding walks *Phys. Rep.* **103** 225
[48] Haus J W and Kehr K W 1987 Diffusion in regular and disordered lattices *Phys. Rep.* **150** 263
[49] Bouchaud J-P and Georges A 1990 Anomalous diffusion in disordered media: statistical mechanisms, models and physical applications *Phys. Rep.* **195** 127
[50] Hughes B D 1995 *Random Walks and Random Environments* vol 1 (Oxford Science Publ., Clarendon)
[51] Dean D S, Drummond I T and Horgan R R 2007 Effective transport properties for diffusion in random media *J. Stat. Mech.* **2007** 07013
[52] Bogachev L V 2006 *Random Walks in Random Environments* (*Encyclopedia of Mathematical Physics*) vol 4 ed J-P Francoise, G Naber and S T Tsou p 353
[53] Valov A, Levi N and Meerson B 2024 Thermally activated particle motion in biased correlated Gaussian disorder potentials *Phys. Rev. E* **110** 024138
[54] Reichhardt C and Reichhardt C J O 2014 Active matter transport and jamming on disordered landscapes *Phys. Rev. E* **90** 012701
[55] Licata N, Mohari B, Fuqua C and Setayeshgar S 2016 Diffusion of bacterial cells in porous media *Biophys. J.* **110** 247
[56] Zeitz M, Wolff K and Stark H 2017 Active Brownian particles moving in a random Lorentz gas *Eur. Phys. J. E* **40** 23
[57] Santillan D 2023 Dispersion of run-and-tumble microswimmers through disordered media *Phys. Rev. E* **108** 064608
[58] Mattingly H H 2025 Coarse-graining bacterial diffusion in disordered media to surface states *Proc. Natl Acad. Sci. USA* **122** e2407313122
[59] Kalaj S, Marinari E, Oshanin G and Peliti L 2025 A simple model of a sequence-reading diffusion: non-self-averaging and self-averaging properties *New J. Phys.* **27** 043022
[60] Zwanzig R 1992 Diffusion past an entropy barrier *J. Phys. Chem.* **96** 3926
[61] Bauer M, Godec A and Metzler R 2014 Diffusion of finite-size particles in two-dimensional channels with random wall configurations *Phys. Chem. Chem. Phys.* **16** 6118

[62] Montroll E W and Weiss G H 1965 Random walks on lattices *II J. Math. Phys.* **6** 167
[63] Bedeaux D, Lakatos-Lindenberg K and Shuler K E 1971 On the relation between master equations and random walks and their solutions *J. Math. Phys.* **12** 2116
[64] Lifshits I M, Gredeskul S A and Pastur L A 1988 *Introduction to the Theory of Disordered Systems* (Wiley-VCH)
[65] Lindenberg K and West B J 1986 The first, the biggest and other such considerations *J. Stat. Phys.* **42** 201
[66] Redner S 2001 *A Guide to First Passage Processes* (Cambridge University Press)
[67] Metzler R, Oshanin G and Redner S ed 2014 Oshanin and S *First-Passage Phenomena and Their Applications* (World Scientific)
[68] Bénichou O and Voituriez R 2014 From first-passage times of random walks in confinement to geometry-controlled kinetics *Phys. Rep.* **539** 225
[69] Grebenkov D, Metzler R and Oshanin G ed 2024 *Target Search Problems* (Springer)
[70] Weiss G H 1966 First passage time problems in chemical physics *Adv. Chem. Phys.* **13** 1–18
[71] Lifson S and Jackson J L 1962 On the self-diffusion of ions in a polyelectrolyte solution *J. Chem. Phys.* **36** 2410
[72] Festa R and d'Agliano E G 1978 Diffusion coefficient for a Brownian particle in a periodic field of force *Physica A* **90** 229
[73] Kalnin J R and Berezhkovskii A M 2013 On the relation between Lifson-Jackson and Derrida formulas for effective diffusion coefficient *J. Chem. Phys.* **139** 196101
[74] Gillespie D T 2007 Stochastic simulation of chemical kinetics *Ann. Rev. Phys. Chem.* **58** 35
[75] Doyle P G and Snell J L 1984 *Random Walks and Electric Networks* (American Mathematical Soc.)
[76] Mejia-Monasterio C, Oshanin G and Schehr G 2011 First passages for a search by a swarm of independent random searchers *J. Stat. Mech.: Theor. Exp.* **2011** 06022
[77] Mattos T G, Mejia-Monasterio C, Metzler R and Oshanin G 2012 First passages in bounded domains: When is the mean first passage time meaningful? *Phys. Rev. E* **86** 031143
[78] Karlin S 2014 *A First Course in Stochastic Processes* (Academic)
[79] van Kampen N G 2007 *Stochastic Processes in Physics and Chemistry* (North-Holland Personal Library, Elsevier)